PIXE ANALYSIS OF ADJACENT ELEMENTS

BY

NKARO ALDEFRIDA MATETA (nee MASHILO)

Dissertation presented in partial fulfilment of the requirements for the degree of

MASTER OF SCIENCE

to the

DEPARTMENT OF CHEMISTRY
UNIVERSITY OF CAPE TOWN

Promoter: Dr. M. Peisach
Co-promoter: Mr. M. A. B. Pougnet

SEPTEMBER 1991

To my sons, Monageng and Ramakatsa

Acknowledgements

I am indebted to a number of people without whose help, assistance and guidance this work would not have been possible:

Dr M. Peisach, my promoter, of the Nuclear Analytical Chemistry Division, Van de Graaff Group, National Accelerator Centre, for his guidance, active participation, continuous support, constant encouragement and stimulating discussions throughout his supervision of this investigation;

Mr. M. A. B. Pougnet, my co-promoter, for the fruitful discussions and advice;

Dr. D. Reitmann, Director of the National Accelarator Centre, and Dr. W. R. McMurray, head of the Van de Graaff Group, for the use of the facilities at the National Accelarator Centre;

Messrs H. Schmitt, G. Ackermann, P. Groenewald, T. Swart and the technical personnel of the Van de Graaff Group, for their friendly assistance and efficient operation of the accelerator and maintenance of laboratory equipment;

Mr P. Groenewald, for his patience and expert preparation of some of the drawings;

Mr S. Hendricks, for the photographic work;

Mr T. K. Marais, for his assistance and helpful comments during the development of computer programs;

Drs R. Pretorius and S. Tapper for the proof-reading of this manuscript;

My husband, parents and the rest of my family, for their moral support and encouragement.

SUMMARY

Proton induced X-ray emission (PIXE) analysis depends on the accurate stripping of the peaks of individual X-rays from the X-ray energy spectrum produced by the bombardment of a target material with charged particles. The energy separation between the K_β X-ray of element Z and the K_α X-ray of element (Z + 1) increases with increasing Z. Accordingly, for adjacent lower Z elements, there is an overlap in energies between these two X-rays, and hence interference may be caused by one element in the determination of the other.

The purpose of this investigation was to determine the extent of such possible interferences and to evaluate the accuracy and precision of the determination of adjacent elements, especially when one of the pair is present in overwhelming concentrations.

Two elemental pairs, potassium-calcium, of biological significance, and vanadium-chromium, of metallurgical significance, were studied in detail. Mixtures of stock solutions of the two elements of each pair were made to provide samples with elemental ratios of the minor component decreasing from 10^{-1} to 10^{-4} relative to the major one. A minimum of five of these samples were prepared on thin foils as well as on thick target pellets for each concentration level, and the PIXE spectra were recorded under bombardment with protons of 3 MeV. The spectra were analysed off-line by the program AXIL, which, in cases where the minor component could not be visually identified in the spectrum, was *forced* to evaluate the concentrations of both components. Under these conditions, low levels of the minor component were reported even though the component could not be resolved.

All samples, the spectra of which showed the presence of both elements of the elemental pairs, could be analysed in mg/g concentration range. The precision and accuracy of such analysis were acceptable, except in the case of pellets onto which solutions containing both potassium and calcium were deposited. Chromatographic separation of potassium from calcium during the diffusion of the solution in the pellet matrix gave unacceptably erroneous results.

When the concentration of the major component exceeded that of the minor by a factor of 200 or more, the presence of the minor component could no longer be recognised in the spectra. When such spectra were analysed by AXIL, *forcing* the program to determine both elements, results were a reflection of background levels in the energy region of the expected peak. It could therefore be concluded that the determination of the minor component in the presence of the major one for adjacent elements by PIXE is inaccurate for relative concentrations less than 1 : 200.

CONTENTS

Chapter 1

INTRODUCTION

1.1 Introduction

Since the discovery of positive evidence of the emission of characteristic X-rays in 1910 [Ba 11], the application of X-ray emission has been widespread. The establishment of the relationship between the wavelength (and hence the energy) and the atomic number [Mo 13],

$$\lambda \propto 1/Z^2 \tag{1.1}$$

led to the use of this technique for the identification of elements. The proportionality constant in equation (1.1), depends on the X-ray series, K, L, M etc and on the particular line in that series. Although the equipment was relatively economical and reliable, the technique never found widespread use in the early years after its discovery, because of the experimental requirements of high vacuum, the use of electrons for excitation and the need for the target to be conducting. The same problems were encountered in later years [Al 25, Vo 32, Co 25], when X-rays were used as the excitation medium.

It was not until the late 1950's and early 1960's, that X-ray emission found routine application for elemental analysis, with the use of wavelength dispersive spectrometers, in which the wavelengths were separated by Bragg diffraction from a single crystal.

It is interesting to note that when the relative advantages of electrons, pro-

tons and X-rays for X-ray excitation were compared in 1964 [Bi 64], X-rays were chosen as being the most practical at that time. However, two major events were responsible for renewed interest in charged particle-induced X-ray emission (PIXE);

1. the introduction of high-resolution Si(Li) detectors for energy dispersive X-ray analysis, and,
2. the phenomenal detection limits for elemental analysis with 3 MeV protons reported in the early 1970's, [Jo 70, Jo 72].

1.2 X-ray yields

PIXE is concerned with the measurement of characteristic X-rays produced when a target is bombarded with charged particles. The X-ray yield, $Y_o(Z)$ [in *counts per second*], for an element Z and atomic mass A_Z, in a thin film of areal density $M_a(Z)$[in $\mu g.cm^{-2}$], bombarded with charged particles of energy E_o [in MeV] is given by, [Pi 91]

$$Y_o(Z) = N_p M_a(Z) \sigma_I(Z,E) \omega_z b_z \epsilon_z N_A \Omega / A_z \tag{1.2}$$

where

N_p is the bombarding current [in *particles per second*],

$\sigma_I(Z,E)$ is the ionisation cross section of element Z, at energy E,

ω_z is the fluorescence yield,

b_z is the branching ratio,

ϵ_z is the efficiency for the measured X-ray,

N_A is Avogadro's number,

Ω is the solid angle subtended by the detector, and

A_z is the atomic mass of element Z.

A constant $k(Z)$ which includes geometrical factors and yield constants can be defined as:

$$k(Z) = \omega_z b_z \epsilon_z N_A \Omega / A_z \tag{1.3}$$

then

$$Y_o(Z) = N_p M_a(Z) k(Z) \sigma_I(Z, E) \tag{1.4}$$

A simple calculation of the ionisation cross-section [Me 69], using the Plane Wave Born approximation and wave-functions similar to hydrogen gave the result,

$$\sigma_I(Z, E) = 8\pi r_o^2 [\frac{z^2}{Z_{eff}^4}][\frac{f(\eta, \theta)}{\eta}] \tag{1.5}$$

where

r_o is the Bohr radius,

z is the charge on the bombarding particle,

Z_{eff} is the effective nuclear charge on the target atom, and

η, θ and $f(\eta, \theta)$ are dimensionless tabulated parameters [Me 69], related to the type of X-ray, K, L, M. . . etc.

This approximate expression agrees satisfactorily with experimental values for high velocity bombarding particles. Modifications of equation 1.5 were made [Br 81] to include the effect of Coulomb field, (C), perturbation of the atomic stationary states, (PSS), the relativistic effects, (R), and energy loss during collision, (E), to yield the so-called ECPSSR relationship. Cross sections based on the ECPSSR equation have been tabulated [Co 85], for K, L_1, L_2 and L_3 subshells and bombarding particles of protons and helium ions.

From the above, it is evident that at constant bombarding energy, the yield of X-rays is a smoothly varying function of the atomic number. Accordingly the elemental concentrations of many elements may be determined simultaneously from a single X-ray spectrum, even if the absolute concentration of only one component can be determined or is known.

When thick targets are used, i.e. targets in which the bombarding beam is stopped, the yield equation has to be modified to take into account the decrease in the energy of the bombarding particle along its path through the sample matrix. Equation 1.2 can then be rewritten to give the yield of the required X-ray, Y(Z) as

$$Y(Z) = \frac{Y_o Z}{(M_a)_{total} \sigma(Z_1 E_o)} \int_o^{E_o} \frac{\sigma_I(Z_1 E) T(E)}{S(E)} dE \tag{1.6}$$

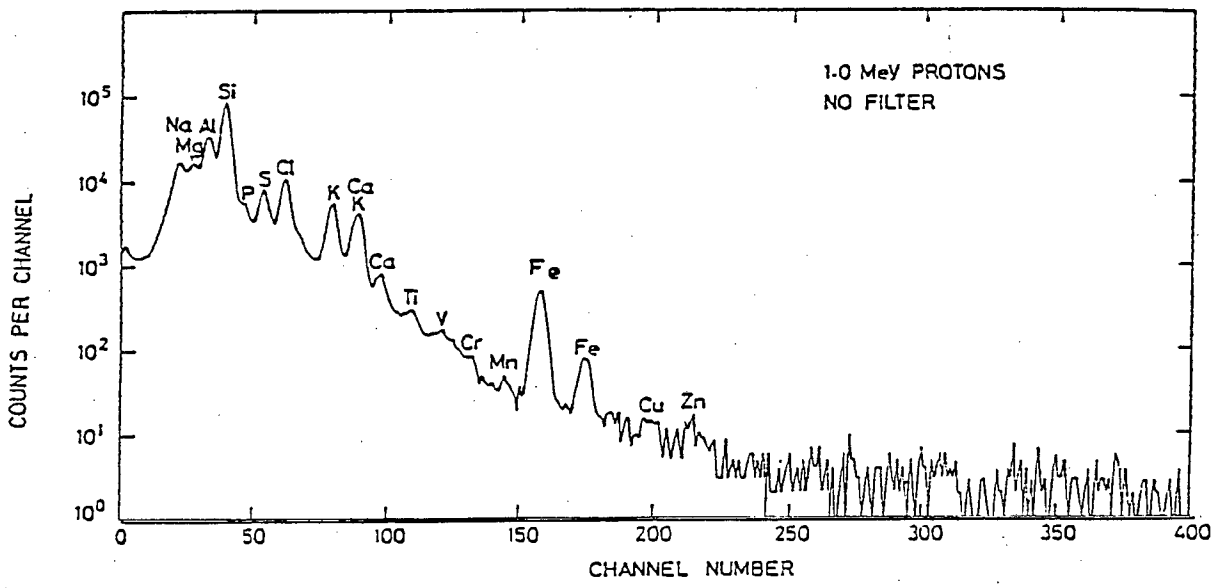

Figure 1.1: Spectra from the skin of golden delicious apples showing the elements that can be determined using PIXE, [after Me 80].

where

$(M_a)_{total}$ is the total areal mass of the target material,

$T(E)$ is the transmission factor which accounts for the absorption of the measured X-rays within the target material and is dimensionless and

$S(E)$ is the stopping power of the matrix [in eV *per unit thickness*].

The ionisation cross section at the surface of the of the target where no energy loss has occurred is $\sigma(Z_1 E_o)$.

1.3 The relative concentration ratios

The analytical evaluation of the PIXE spectrum, (see Figure 1.1),

[Me 80], involves the determination of the areas under each peak, since the

areas are proportional to the X-ray yields. In most applications, overlapping X-ray energies of different elements are encountered, imposing a burden on the interpretation and evaluation of the data.

When one element in a pair under consideration is in an appreciable concentration, it may be used as the basis of comparison for expressing relative concentration ratios. When the spectrum of a specimen is analysed, the integrated peak counts for one element in the sample relative to that of another is given by,

$$R = \frac{Y_o(Z_1)}{Y_o(Z_2)} = \frac{M_a(Z_1)k(Z_1)\sigma_I(Z_1,E)}{M_a(Z_2)k(Z_2)\sigma_I(Z_2,E)} \tag{1.7}$$

Since both elements are bombarded with the same flux, and measured with an efficiency which effectively remains constant, [Ak 74], over the energy range 3-20 keV. The values of the cross-section, σ_I, depend on Z^4, since all other factors in equation 1.5 are about equal for the different elements. The count ratio R, is therefore a measure of $M_a(Z_1)/M_a(Z_2)$, i.e the relative elemental concentration.

1.4 Mathematical techniques for spectrum analysis

Improvements in detection and data recording systems in recent years have led to such amounts of information that manual analysis of X-ray spectra has become difficult. Not only can the total number of peaks present in a spectrum be very large, but also the unbiased resolution of composite peaks and the reliable estimation of the errors in the peak parameters can be tedious. There is therefore a strong need for mathematical techniques for determining the intensities of measured X-rays. A number of techniques is available for generating functions to represent the background and the peaks.

1.4.1 Single peak stripping

A spectrum may be "stripped down" [Qu 72] using previously measured information about background and line shapes generated with calibrated standards. One such program is SAMPO, which was originally written for handling gamma-ray spectra [Ro 69,Gi 84].

The spectrum is divided into regions according to the intensities of the full energy peaks in each region, followed by sequential stripping in each region. However, the disadvantage of this technique is the accumulation of errors in each consecutively stripped peak. In the evaluation of data for the determination of pottery and glasses, it was found [Gi 84] that Fe K_α yield could not be used for the normalization of PIXE elemental data because of the presence of manganese. The energy of the Fe K_α X-ray is 6.403 KeV and that of the Mn K_β is 6.490 KeV. The energy difference between these two X-rays was less than the resolution of the detector, and hence the computer program treated the data as a single peak. Resolution of these two peaks was therefore impossible because the computer program was not designed to consider other spectrum peaks as originating from the same element and thus could not normalise the contribution of the Mn K_β counts on the basis of the Mn K_α yield. Similar interferences occurred in the case of the K K_β X-ray with that of the Ca K_α [Gi 84].

1.4.2 Analytical fitting using measured standards

Programs written specifically for PIXE differ from each other only in the analytical expression for the peak shape. All programs rely on a Gaussian shape to describe the main spectral contribution. Tailing effects at the low and high energy sides, and background are treated differently.

The use of a library of measured spectra enables the correct parameters to be selected and corrections are made for escape peaks, pileup, X-ray absorption and

detector characteristics. The comparison of the programs most commonly used and based on measured standards is given in Table 1.1, [Ca 86, Jo 88].

1.4.3 Analytical fitting using physical parameters

A different approach was adopted [Va 77] for the deconvolution of X-ray spectra, using a non-linear least-squares fitting program AXIL. The program is based on an algorithm [Ma 63] which ensured convergency of the minimisation process, finds the minimum of chi-squared and combines a gradient search with an analytical solution by linearisation of the fitting function. The program provides an analysis report of the nett peak intensities (corrected for background and peak overlap) of the different elements analysed.

Figure 1.2 [Va 77a] shows the general flow of events for the AXIL program. The least-squares fitting program divides naturally into two parts;

1. the first is to locate the peaks in the spectrum corresponding to energies stored in the library of the computer from a supplied calibration equation (see INPUT in figure 1.2)

2. the second is to fit the peaks with fitted peak shape and background function using peak intensities of the elemental spectra from a stored library (see SUBROUTINE INITP in figure 1.2)

As is the case with other programs, the main energy peaks are fitted with Gaussian distributions to which the appropriate background contribution is added. The background contribution is expressed as a polynomial, the coefficients of which can, if necessary, be adjusted by the operator.

Table 1.1: Programs most commonly used for analytical fitting of PIXE spectra

Program	HEX	SESAMX	GUPIX	PIXAN
Reference	[Jo 82, Ka 77]	[Ha 77]	[Ma 84]	[Cl 83, St 76]
Fit procedure	(L[#] + NL[&])/LSF[$]	L/LSF	NL/LSF	NL/LSF
Background	Analytical model	Analytical model	Digital filter	Polynomial or iterative removal
Peak shape	Gaussian + step on left	Gaussian + exponential tail	Gaussian exponential step	Gaussian + exponential tail + step between K_α and K_β
Escape peaks	parametized	own parametization	parametized	prestripped
K X-ray intensities	[Sc 74]	measured	[Sc 74]	[Sa 74]
Thickness correction to relative intensities	no	no	no	yes
Pileup peaks	[Jo 82]	energy dependent version of [Jo 82]	[Jo 82]	[Jo 82]

[#]Linear

[&]Non-linear

[$]Least-squares fitting

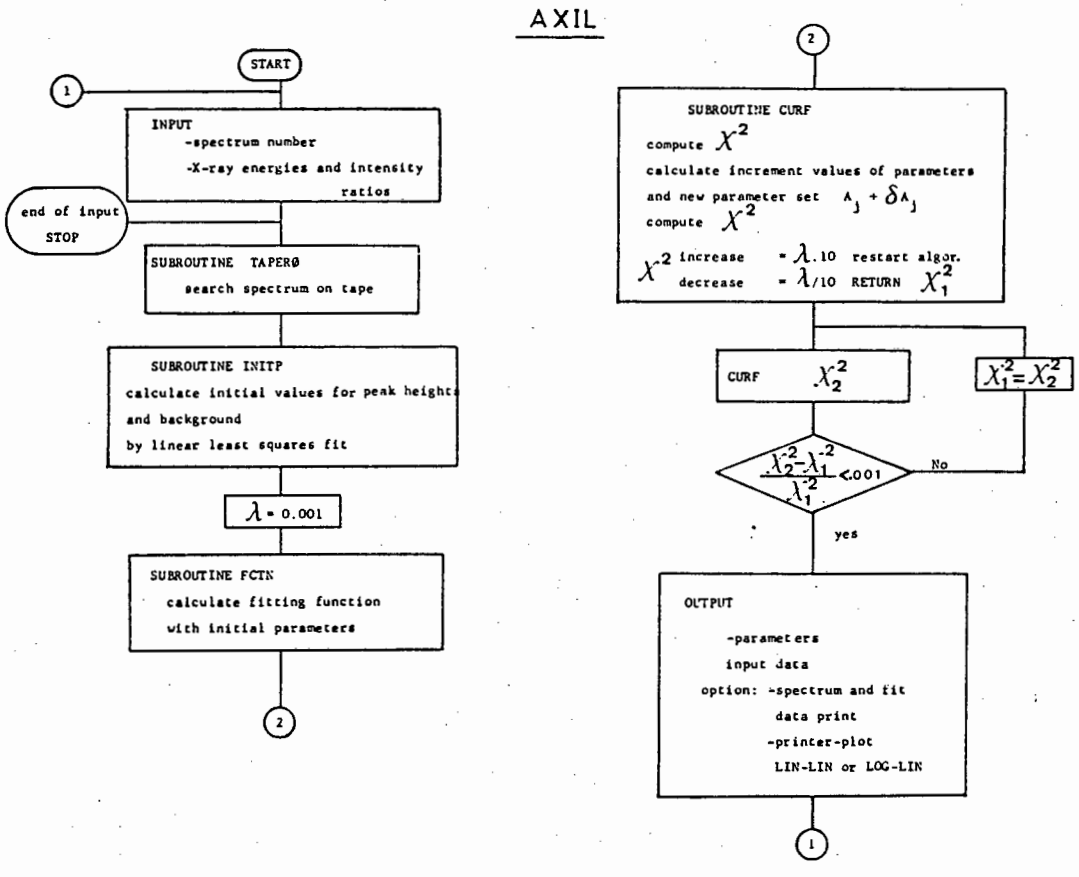

Figure 1.2: General flow chart of the computer program.

1.5 The X-ray background

The most significant factor limiting the sensitivity of PIXE measurements is background radiation. When the accelerated charged particles traverse a target, some background radiation is emitted from the matrix and surroundings of the target together with the characteristic X-rays from the component elements. A typical spectrum is shown in fig. 1.3.

In the spectrum shown, the characteristic X-ray peaks are superimposed on a continuous background of electromagnetic radiation. This continuous background

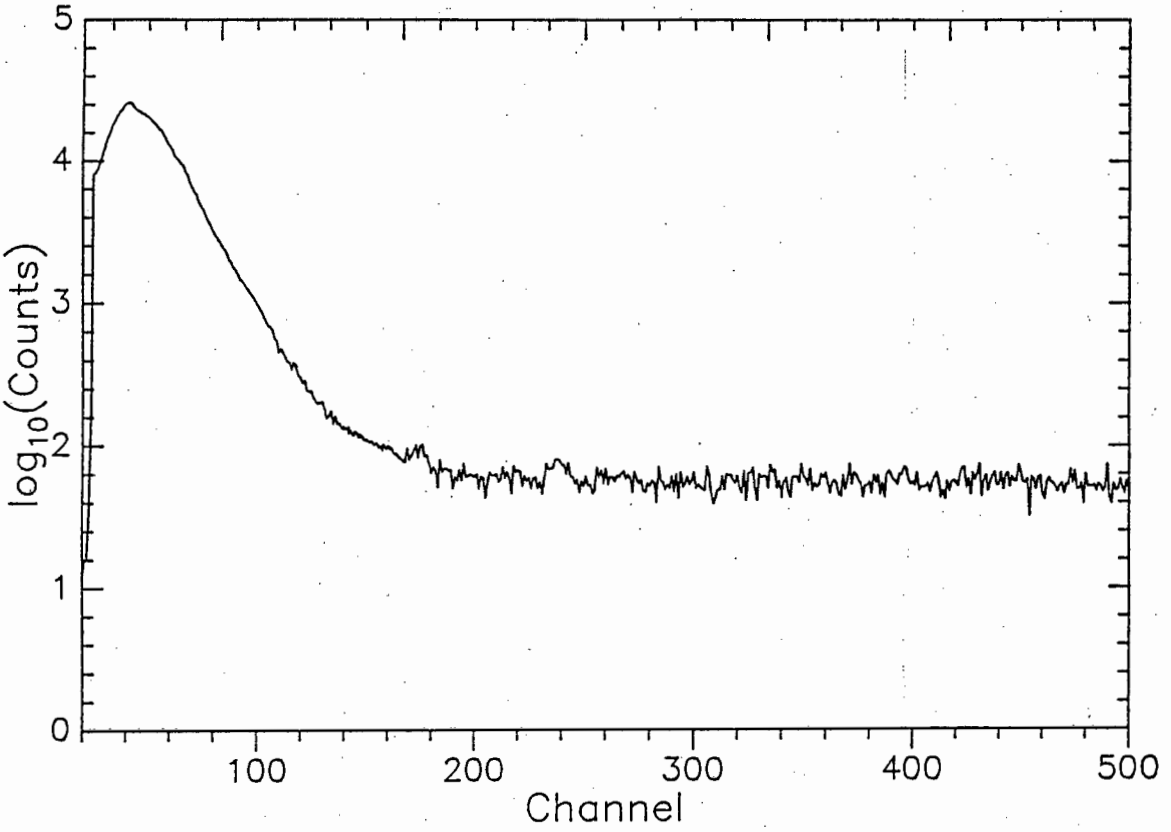

Figure 1.3: A typical background spectrum obtained from the bombardment of a urea pellet with 3 MeV protons

is relatively lower in intensity than that encountered by other methods of X-ray excitation, such as exposure to electromagnetic radiation from X-ray tubes, radioactive sources or electron bombardment, [Yo 73]. The continuous background radiation observed from the spectrum was ascribed as due to bremsstrahlung from secondary electrons and from projectile.

On the low-energy side of the spectrum, the most significant contribution to the background probably comes from secondary electrons, [Fo 74, Is 76]. The production cross section for this process is given by, [Re 80]

$$P = \frac{d\sigma_{br}}{d(\hbar\omega)d\Omega} = \frac{2}{\pi}\,\frac{Ze^2}{\hbar c}\cdot\left(\frac{e^2}{m_e c^2}\right)^2\,\left(\frac{c}{v}\right)^2\,\frac{1}{h\omega}\,ln\left(\frac{4E_e}{\hbar\omega}\right)\frac{sin^2\theta_{br}}{(1-\beta cos\theta_{br})^4} \qquad (1.8)$$

where

ω is the laboratory solid angle subtended by the detector,

m_e, e, v and E_e the mass, charge, velocity and energy E_e of the secondary electron, respectively,

$\hbar\omega$ the photon energy, and

θ_{br}, the angle at which the bremsstrahlung photon is emitted relative to the direction in which the electron is travelling. Secondary electron bremsstrahlung decreases rapidly above an X-ray energy of:

$$E_x \approx \frac{4m_e}{M}E \tag{1.9}$$

which is the maximum energy transfer from a projectile of mass M and energy E to a free electron of mass m_e. For a bombarding proton energy of 3 000 keV, the secondary electron bremsstrahlung maximum energy is about 6.5 keV.

1.6 Sensitivity of PIXE analysis

The lowest concentration of an element that can be determined by an analytical method is the sensitivity of the method and, in PIXE, is measured by the lowest number of X-ray counts under a peak that can statistically be distinguished from the background. Since every peak is measured against a background continuum, the intensity of the background will determine the attainable sensitivity. This relation has been represented mathematically by [Cu 68] as,

$$C_{nett} = r\sqrt{C_{bg}} \tag{1.10}$$

where C_{nett} and C_{bg} refer respectively to the nett integrated counts under the the spectrum peak of interest and the integrated background under the same peak.

Three levels have been defined based on the above equation for determining the lowest levels at which a given element may be detected;

1. A concentration region where the nett peak is sufficiently precise to enable quantitative analysis to be carried out with a relative standard deviation of less than 10%. In this region $r \geq 10$.

2. A lower level of concentration where the nett peak is sufficiently intense for qualitative analysis but where quantitative analysis become inexact. In this region $10 > r \geq 3.29$.

3. The lowest concentration region where the definition of the nett peak is indistinct and qualitative analysis becomes unreliable. In this region $3.29 > r \geq 1.64$.

Most workers accept as a rule of thumb, that the sensitivity is given by,

$$C_{nett} = 3\sqrt{C_{bg}} \tag{1.11}$$

Since the yield of X-rays increases with the bombarding energy, the attainable sensitivity can improve with increased energy. Thus for analysis the optimum bombarding energy still has to be determined experimentally in order to give the best compromise between increased yield and increased background, even though the energy at which the maximum cross section for X-ray production can be calculated.

By calibration with standard materials, the sensitivity factor, S, can be evaluated for the X-ray under consideration, and is given by

$$S = \frac{C_o}{W_o} \tag{1.12}$$

for a fixed bombarding charge, where C_o nett counts were obtained from the known content of W_o μg of the element. At the sensitivity limit, the lowest mass that can be determined is W_{min} and

$$C_{nett} = W_{min} \times \frac{C_o}{W_o} = W_{min}S \tag{1.13}$$

Hence by substitution in equation (1.10)

$$W_{min} = \frac{3.29}{S}\sqrt{C_{bg}} \tag{1.14}$$

for the same fixed bombarding charge used to define S in equation (1.12).

1.7 Spectral interferences

The limited spectral resolution of energy dispersive systems makes line interference unavoidable when X-ray energies are close together. Fortunately, mathematical techniques (see section 1.4) are available to strip overlapping peaks in a spectrum and to obtain separated peak intensities. However, the accuracy of such stripping programmes is affected by the statistical precision of the measurement, the number of peaks in the overlapping region and their relative intensities. In particular, the precision of determining the intensity of a small peak in the vicinity of an intense one is generally rather poor.

In the energy region of about 3 to about 7 keV, the main source of interference due to overlapping energies of X-rays is the occurrence of low energy L X-rays and of K_β X-rays of element Z with energies lying close to that of the K_α X-ray of element (Z+1). This energy difference, Δ, can be expressed as:

$$\Delta = \left|(E_{K_\beta})_Z - (E_{K_\alpha})_{Z+1}\right| \tag{1.15}$$

and the values of Δ are shown plotted as a function of the atomic number in Figure 1.4, for the atomic-number range $14 \leq Z \leq 30$. The occurrence of L X-rays depends on the composition of the sample, so that interference from L X-rays falls outside the scope of this investigation.

At present, the energy resolution, given by the full width at half the maximum height, of most good Si(Li) detectors is of the order of 150 eV. In Figure 1.2, the elements Cl, Ar, K, Ca, Sc, Ti, V, Cr, Mn and Fe lie in the region where mutual interference between adjacent elements occurs and where separation of their spectral peaks may not be observed.

Mutual interference from elemental pairs is expected to be most severe when the concentration of one of the elements is overwhelmingly large relative to that of the other. In the present investigation the relative concentration ranges over which each of the two elements in the element pairs can be determined separately, have been studied, and in particular the minimum relative concentration that can still

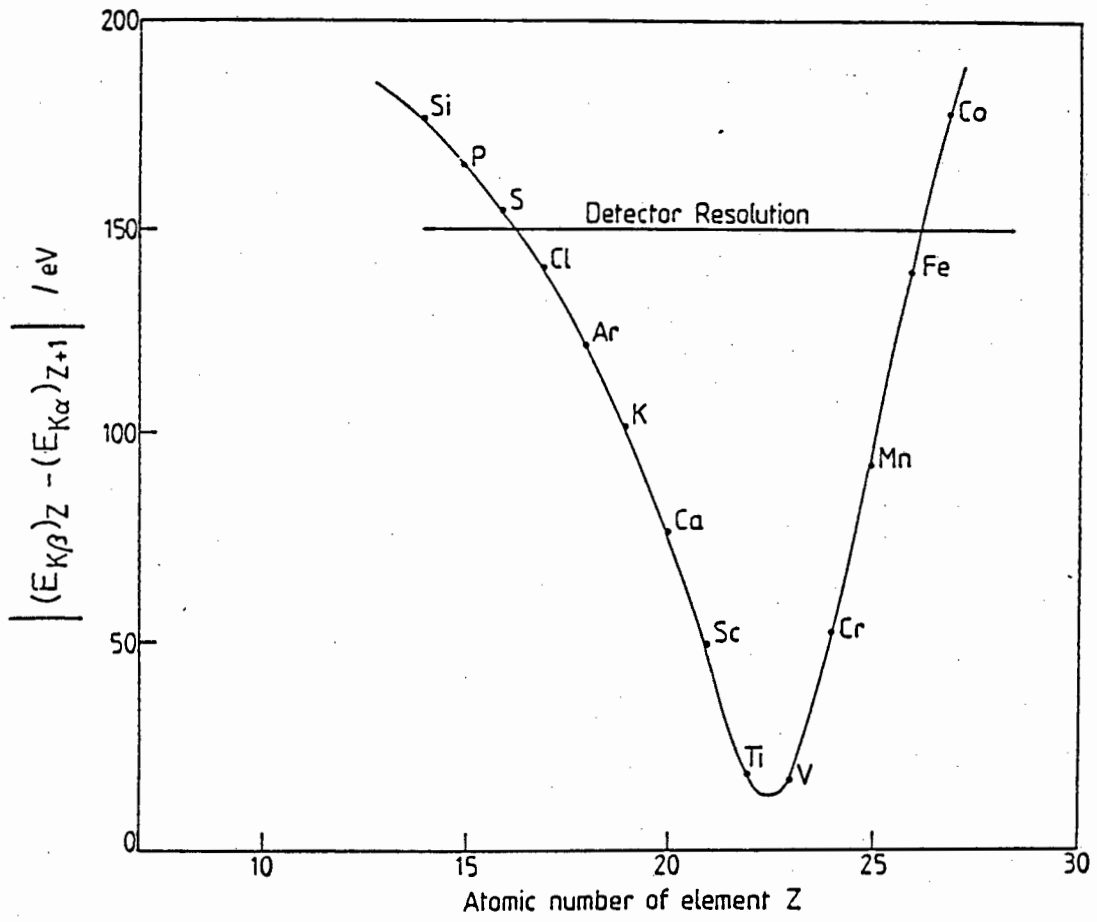

Figure 1.4: Energy differences between the K_β X-ray of one element Z, and the K_α X-ray of the next (Z+1) as a function of the atomic number Z.

be measured of the low concentration component, has been determined.

In the interpretation of the data for the analysis of the Mn-Fe elemental pair, in spectra obtained from the standard reference material Orchard Leaves it was found [Ca 86] that when the intensity of the Mn K_α X-ray was strong compared to that of the Fe K_α X-ray, analytical results for manganese were reproducible with the relative precision of 1%. However, the precision deteriorated as the intensity of the manganese X-ray decreased relative to that of the iron. It was significant that difficulties were experienced [Ca 86] in determining the intensity of the Cr K_α X-ray, because not only does its peak occur on the low energy tail of the peak due to Fe K_α X-ray, but its energy coincides with that of the escape peak from the Fe

K_β X-ray. The precision for chromium determination was poor even though the contribution of the iron escape peak was only about 7% of that of the Cr K_α [Ca 86].

With potassium and calcium, an added difficulty was experienced. The peaks from the K_α X-rays of these elements lie in the bremsstrahlung region of the spectrum, so that in addition to overlapping X-ray energies, a relatively high background is present. This aggravates the precision for determining low concentrations of either of these elements. Thus, in the standard reference material Bovine Liver good precision was obtained for the determination of potassium, which was present in a relatively high concentration while the same data yielded poor results for calcium, the concentration for which was much lower [Ca 86]. When calcium was more concentrated than potassium, as was the case in Orchard Leaves, the reverse was true.

1.8 The purpose of this investigation

It is evident from Figure 1.4 that the pair of elements Ti-V is the pair for which mutual interference would be most severe. Nevertheless, this pair was not selected for investigation because the need to analyse this elemental pair occurs less frequently than the need to determine K and Ca in the presence of each other.The two element pairs, potassium, calcium and vanadium, chromium occur together in biological and metallurgical samples respectively. Unfortunately, each one of them has a special function in a matrix in which it is found, and thus cannot be separated. Even if separation was necessary, it would affect the end results, producing big errors of contamination due to impurities in the chemicals used.

Both potassium and calcium are important mineral elements in fruits and vegetables:
For example, the treatment of the soil with calcium in apple trees result in an increase in the concentration of potassium, which is an important nutrient in apples.

Both vanadium and chromium are important in steels, with essentially separate roles:
Vanadium improves elastic strength and impact resistance in steels, while chromium improves the tensile strength and increases resistance to abrasive wear, with retention of good ductility and fatigue properties.

Accordingly it is often necessary to determine simultaneously both elements of the two element pairs noted above. The extent to which adjacent elements interfere with each other was studied in synthetic mixtures, in which the concentration of first one, and then the other of the elemental pair was systematically changed. Samples prepared in this way were analysed by PIXE in order to determine the lowest relative concentration for which meaningful results could be obtained by this analytical technique.

Chapter 2

EXPERIMENTAL

2.1 Sample preparation

The carbonates of potassium and calcium were used for the study of K-Ca pair. For the investigation of the V-Cr pair, sodium orthovanadate (Na_3VO_4) and potassium dichromate ($K_2Cr_2O_7$) were used. All compounds were of Analytical Reagent Grade.

Stock solutions of 1% by mass of the elements under consideration were prepared by dissolving in 0.1M nitric acid (the carbonates) or water. From these stock solutions, test solutions were prepared by mixing appropriate volumes to give the solutions of the required concentration ratios. The largest errors were expected when measuring volumes less than 20μl, when the expected relative error [Gi 80] was of the order of $\pm$5%. Larger volumes were measured with a better precision. The concentrations of the major components in the test solutions relative to the minor component were 10, 20, 50, 100, 200, 500, 1 000, 2 000, 5 000, 8 000 and 10 000.

In a search for a suitable inert matrix for thick target studies, materials that were tested were starch, commercially available "X-ray mix tablets" and pads of Whatmann filter paper, all of which were discarded because they contained traces of the elements under consideration. Urea contained iron and zinc, which were not detrimental to the investigation. Preliminary experiments were thus carried out using urea as an "inert" matrix.

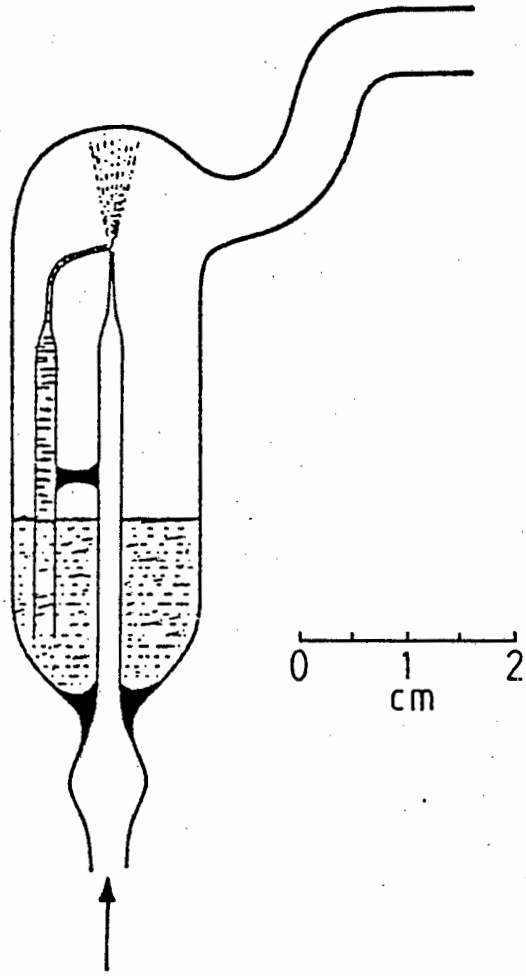

Figure 2.1: Micro-atomiser used for depositing a thin film of dissolved matter on a foil.

Urea powder ('Analar' grade supplied by BDH chemicals, Poole, England), was compressed into tablets of 13 mm diameter and approximately 2 mm thick. Onto these tablets a 20μl volume of the selected test solution was pipetted at the centre of the tablet and the sample was allowed to dry slowly in an oven at 60°C. Fast evaporation resulted in flaking which destroyed the tablet integrity. At least 5 tablets were prepared from each test solution.

Thin samples were prepared on 12μm thick Mylar foils by evaporating an atomised spray of the test solution. The design of the apparatus is shown in Figure 2.1. The gas supply was regulated so as to produce a fine mist which was deposited on a Mylar foil mounted a short distance away from the exit chimney.

Larger drops of spray collected on the walls of the atomiser and returned to the reservoir. Thicknesses of deposits were controlled by the gas pressure and by the duration of spraying. Under constant conditions the deposits were reproducible. With every test solution, a minimum of five samples were prepared. The foils were dried by infra-red heating and stored in a desiccator until required.

2.2 Irradiation and measurement facilities

2.2.1 The irradiation facility and scattering chamber

A proton beam of 3 MeV from the 6 MeV Faure Van de Graaff accelerator was collimated to give a beam with a cross-section of 3.5 mm. The beam current on the target was measured with an Ortec 439 current integrator, and was adjusted in such a way that system dead-time did not exceed 10%. Due to some variations in the proton beam current, the duration of the irradiation was determined by the integrated charge rather than by the clock time. A beam current of approximately 5 nA was used for the analysis of samples.

Irradiations were carried out in a scattering chamber, see Figure 2.2, which was electrically insulated from the beam-line and the detector, so that it served as a self-contained Faraday cup, [Gi 76]. Portholes situated at different angles to the direction of the incident beam, allowed several detectors to be inserted. When not in use, the portholes were covered with transparent perspex plugs through which observations of the inside of the chamber could be made. The target chamber was grounded through a current digitiser for accurate current measurements. Any secondary electrons produced from the target materials are prevented from escaping, by metal disks in the beam tube, perforated to allow the beam to enter. Since the beam entry hole subtends a small solid angle, secondary electron loss through the beam entry port was negligible. Secondary electrons generated by interaction of the beam with the beam tubes were prevented from entering the chamber by a grid charged to -300 V placed in the beam tubes before the collimators outside the

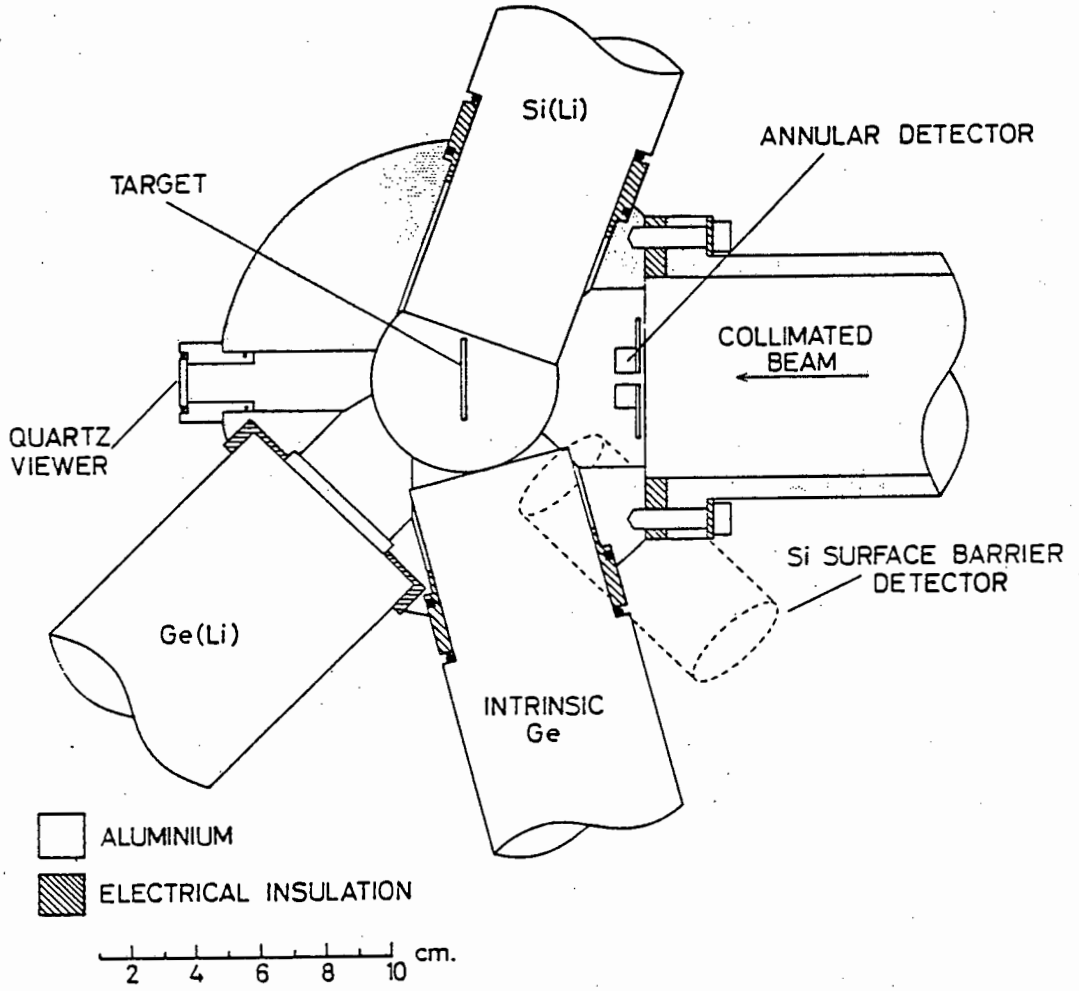

Figure 2.2: Insulated scattering chamber specially designed for analytical use with up to five different detectors.

scattering chamber.

2.2.2 The automatic sample changer

Samples were positioned over holes on the stainless steel ladder, as shown in Figure 2.3. The vertical ladder which had space for ten samples, with an additional vacant position through which the initial beam adjustment was made, was mounted in the target chamber set at an angle of 45° to the beam. The ladder was fitted into the shaft of a motor drive chamber by nylon-grooved wheels on either side see (Figure

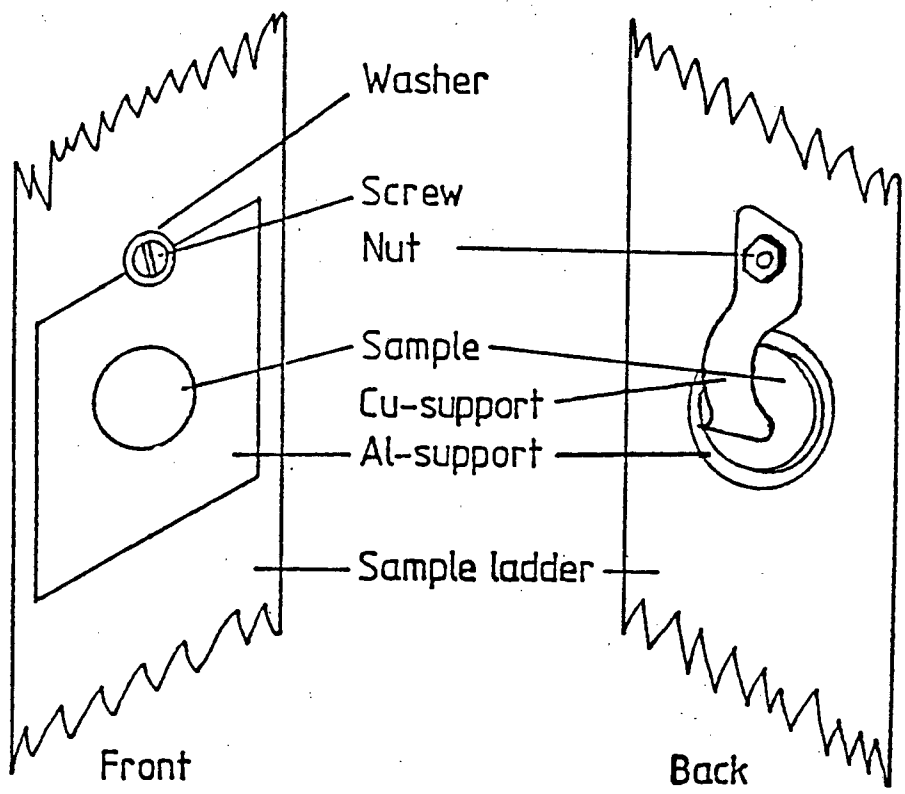

Figure 2.3: Method of mounting samples on the stainless-steel ladder.

2.4). The position of the ladder was remotely controlled by a stepping motor which advanced it at 6.6 μm per step through the centre of the chamber, without breaking the vacuum, [Pe 77].

2.2.3 The electronic measuring system

Figure 2.5 shows a block diagram of the electronic and computation equipment for PIXE measurements. The characteristic X-rays produced by the proton beam were detected by an intrinsic germanium detector, which yielded a pulse amplitude proportional to the energy. The pulses from the detector were amplified by an Ortec model 450 amplifier, capable of handling high count rates without appreciable loss of energy resolution and set to prevent tailing on the low energy side of the peaks. These pulses were then transmitted to a 1024 channel pulse-height-analyser through

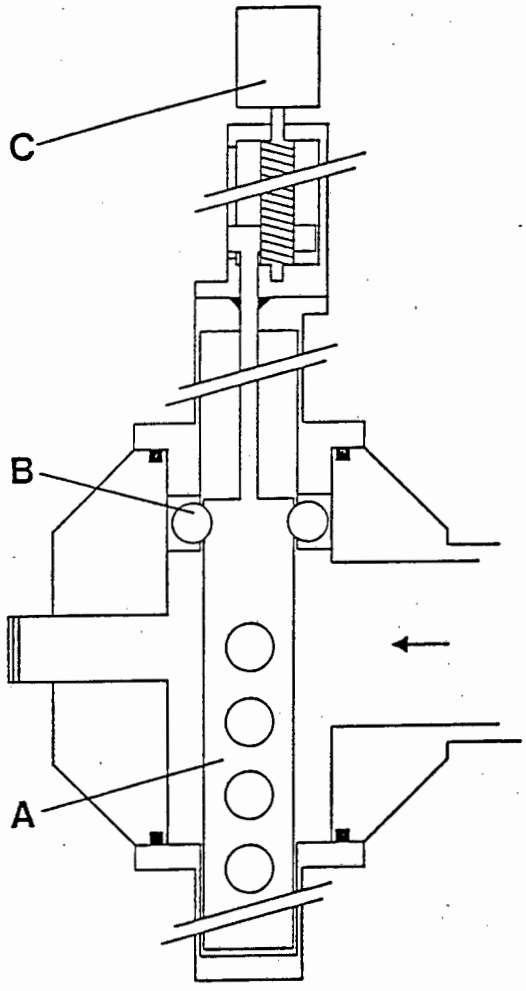

Figure 2.4: Automatic sample changer
A - Sample ladder
B - Nylon positioning wheels
C - Stepping motor.

an analogue to digital converter. A current integrator, set to count for either a pre-determined time or to accumulate a pre-determined total current, automatically switched off the measuring system.

An intrinsic germanium detector oriented at 90° relative to the beam direction, see Figure 2.2, was mounted inside the vacuum of the target chamber. The detector had an active area of 25 mm^2 and a thickness of 5 mm. The resolution at 5.9 keV was 151 eV and at 22.16 keV was 557 eV. The energy was calibrated by a Standard Variable Energy X-ray source (supplied by The Radiochemical Centre, Amersham, England) containing 10mC of ^{241}Am, an alpha emitter, the radiation

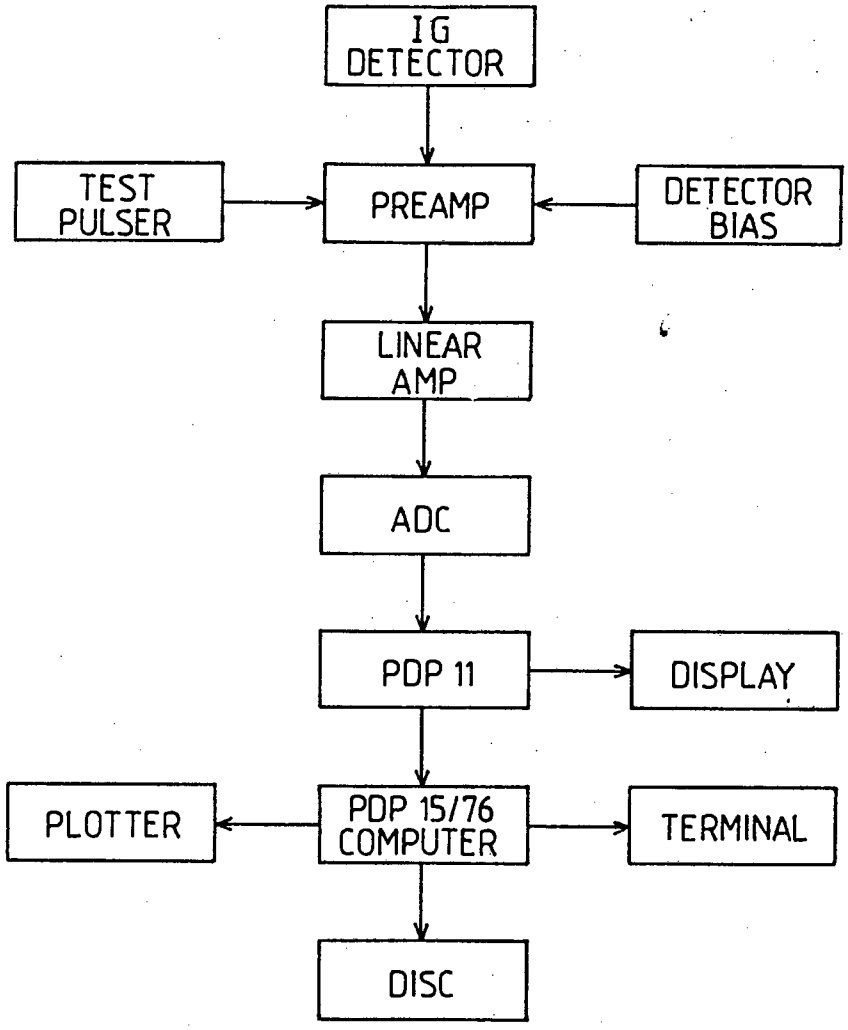

Figure 2.5: Block diagram of electronic and computation equipment for PIXE measurements.

of which could in turn be directed to the sample of Cu, Rb, Mo, Ag, Ba and Tb to yield the X-rays of these elements. Rapid calibration was normally achieved by the use of the Ag $K\alpha_1$ X-ray of 22.162 keV from the X-ray source and the Mn $K\alpha$ X-ray of 5.898 keV from a radioactive source of ^{55}Fe.

A methyl methacrylate absorber, 135 μm thick, was used to prevent backscattered protons reaching the detector. Although this absorber reduced the intensities of the measured X-rays, correction for absorption was unnecessary because the relative extent of absorption was the same for a particular element in every sample pair of the pair under investigation.

2.2.4 The computer system

The pulses from the analogue to digital converter (ADC) fed the PDP computer system, see Figure 2.5, which acted as both the analyser and data reducer. Information about peak position, area and background could be obtained directly . Data were recorded on a magnetic tape for offline analysis. The yields of X-rays were determined by the computer program [Va 77, Va 77a] AXIL, which was run on a VAX 11/750 computer of the National Accelerator Centre near Faure.

Chapter 3

REPRODUCIBILITY AND UNIFORMITY

3.1 Target reproducibility

Different targets, each prepared from the stock solutions were analysed by PIXE to test the reproducibility of target preparation. The results for the thick targets are shown in Table 3.1 and those from thin targets in Table 3.2. The reproducibility of the thick targets was of the order of about 6% while better reproducibility was obtained with thin targets where the values ranged between 1.3 and 3.6%.

3.2 Target uniformity

The uniformity of targets prepared as above was tested by irradiating different spots on the same target material. The results are given in Table 3.3 for thick targets and in Table 3.4 for thin targets for samples containing each of the four elements as a major component. The uniformity of target deposition was repeatedly checked, to ensure that nothing untowards occurred during sample preparation.

Table 3.1: Reproducibility test for thick targets

Target number	Count measured K	Ca	V	Cr
1	98829	77047	145708	175917
2	95505	80979	133830	166199
3	108893	70583	148562	170315
4	106242	81173	135813	170666
5	100200	83299	142856	170298
6	106397	74339	155678	177266
7	105098	74674	157347	195470
8	99060	74375	153622	179494
	102526 ± 4726	77058 ± 4367	146677 ± 8826	175703 ± 9115
	(4.61%)	(5.67%)	(6.02%)	(5.19%)

Table 3.2: Reproducibility test for thin targets

Target number	Count measured K	Ca	V	Cr
1	66318	69205	152961	154065
2	63934	69993	153389	154745
3	61035	68373	153356	152067
4	60443	67346	152100	154498
5	61889	65766	154589	154977
6	61388	-	148748	150190
7	-	-	147792	156249
	62501 ± 2219	68317 ± 1650	151848 ± 2567	153827 ± 2036
	(3.55%)	(2.42%)	(1.69%)	(1.32%)

Table 3.3: Uniformity test for thick targets

100 × Count Ratio of minor to major element			
K/Ca	Ca/K	V/Cr	Cr/V
6.94	5.59	9.20	10.94
6.26	6.98	8.55	10.18
9.52	5.41	9.88	11.75
8.85	5.05	10.00	11.90
7.62	6.16	9.83	11.69
7.84 ± 1.34	5.84 ± 0.75	9.49 ± 0.610	11.29 ± 0.724
(17.10%)	(12.93%)	(6.02%)	(6.41%)

Table 2.4: Uniformity test for thin targets

100 × Count Ratio of minor to major element			
K/Ca	Ca/K	V/Cr	Cr/V
4.38	0.972	1.80	5.12
4.55	0.955	2.17	4.82
4.39	1.14	2.00	5.75
4.32	0.939	2.10	5.74
4.27	0.920	1.82	5.44
4.19	1.03	1.90	4.67
4.36 ± 0.053	0.994 ± 0.033	1.96 ± 0.063	5.25 ± 0.19
(1.22%)	(3.34%)	(3.21%)	(3.62%)

When the relative precision of the count ratio of *thick* targets are compared, targets containing the elemental pair K-Ca were found to be less uniform than those containing V-Cr. The relative precision of the count ratio in the case of V-Cr is of the order of 6%, but is *almost double this amount in the case of K-Ca.* Since the test solution was applied to the centre of the tablet, discrepancies in apparent composition in off centre positions, imply a chromatographic separation of the liquid components laterally and possibly vertically when the test liquid diffuses through the urea matrix. This in turn, would imply that analysis of such tablets would produce results at variance with the known composition of the test liquid. (See Results, section 4.3)

The relative precision of the count ratio of *thin* targets is much better than for thick targets. The relative precision ranging from about 1.2 to 3.6% is acceptable for analysis. Since these were produced by the evaporation of small droplets on an inert film, chromatographic separation could not occur.

Chapter 4

RESULTS AND DISCUSSION

4.1 X-ray spectra

Typical spectra obtained from thin samples on mylar of evaporated solutions containing the pairs of elements in which there is a preponderance of potassium, calcium, vanadium and chromium in the nominal ratio 10 : 1 are shown in Figs 4.1, 4.2, 4.3 and 4.4 respectively. In each figure, the position of the peak from the K_β X-ray of the lighter element is shown in brackets. Spectra from samples containing different elemental ratios are shown in the next section, (Section 4.3). The program AXIL was used to strip the component peaks and to evaluate the peak areas.

Details of the count yields obtained from both elements in the pairs, their count ratios and the relative concentration ratios determined from these data are given in Appendix B.

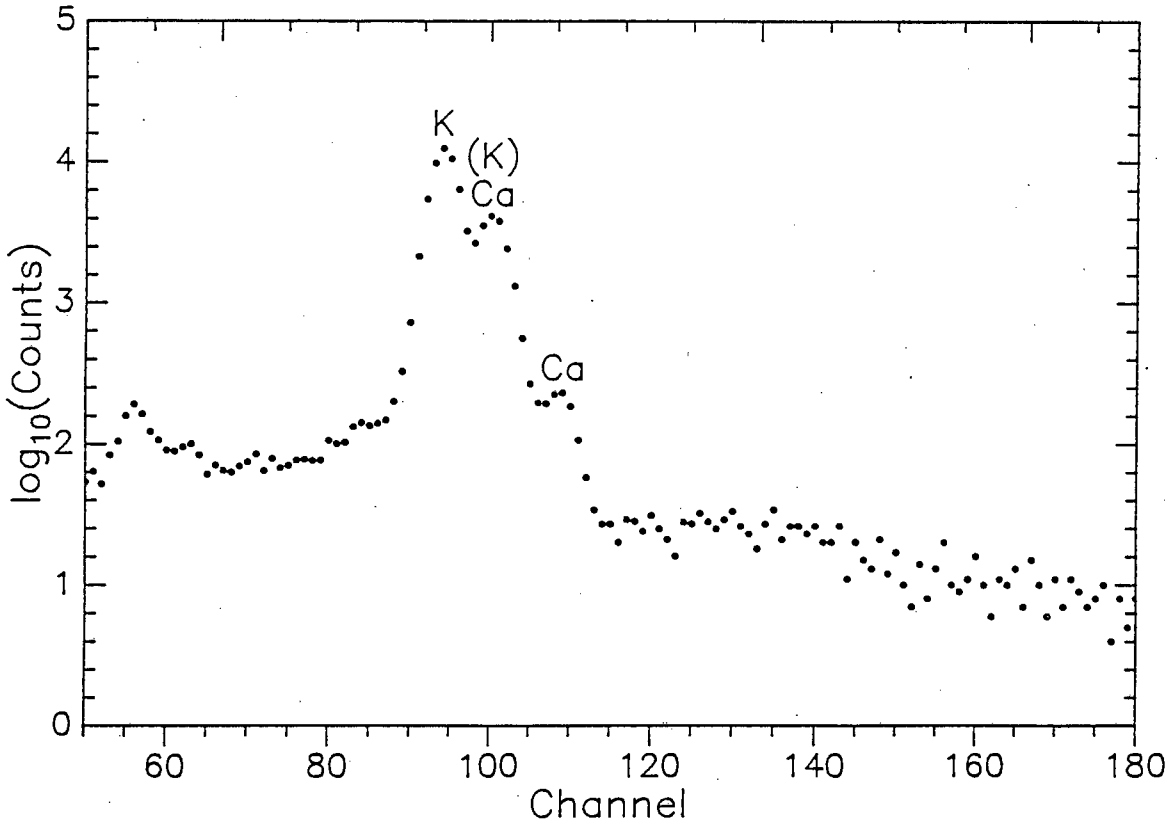

Figure 4.1: Energy spectrum of X-rays from a sample containing a high concentration of potassium.

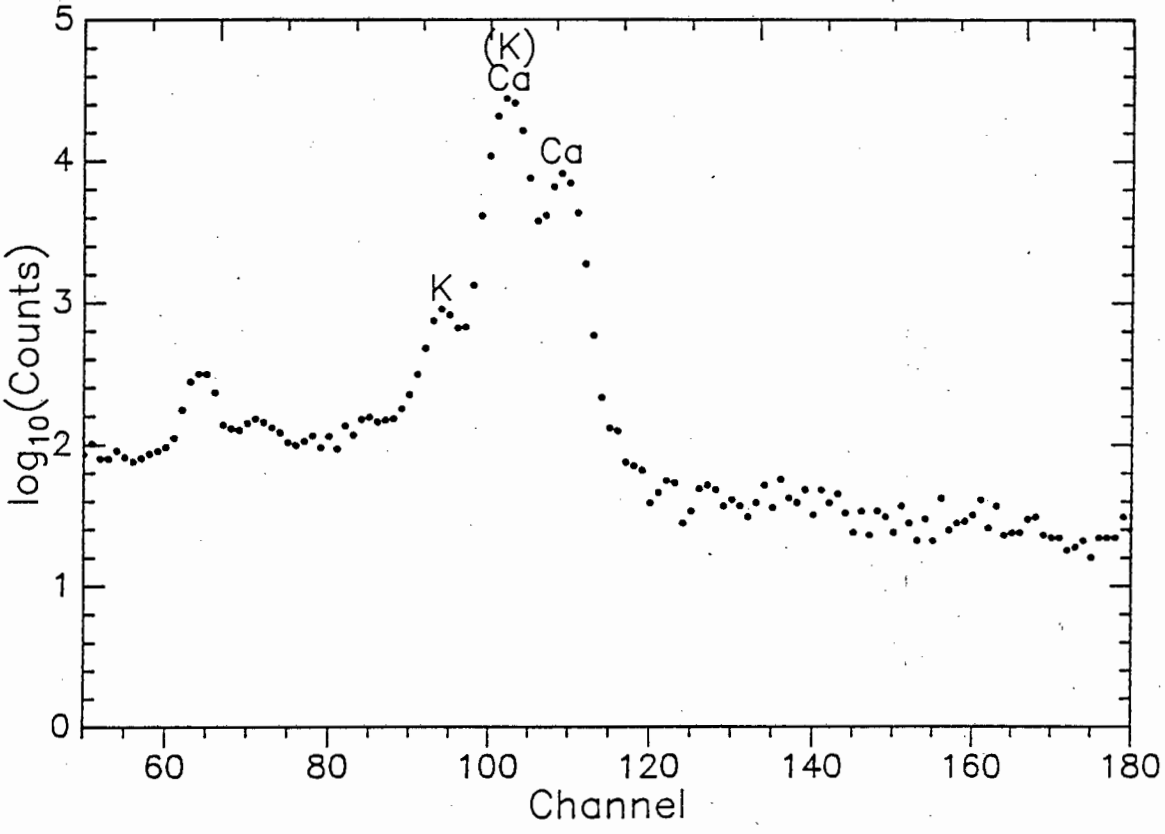

Figure 4.2: Energy spectrum of X-rays from a sample containing a high concentration of calcium.

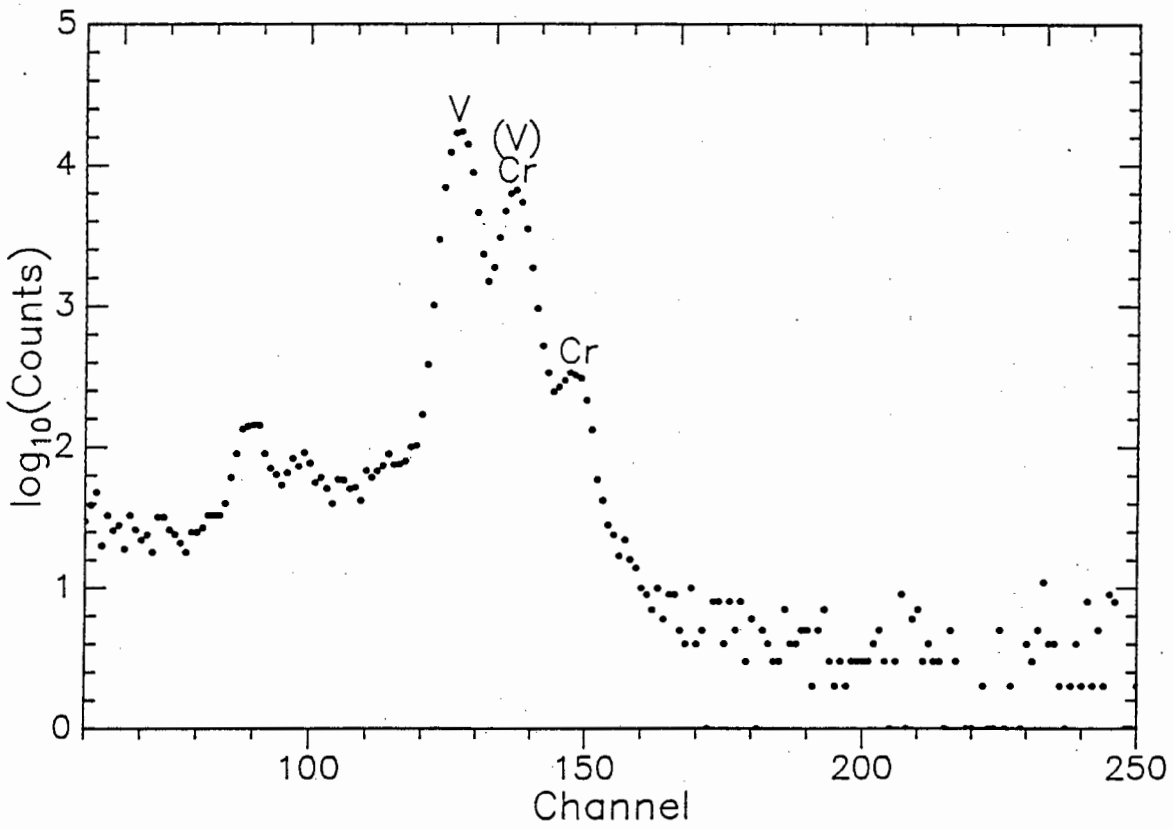

Figure 4.3: Energy spectrum of X-rays from a sample containing a high concentration of vanadium.

4.2 Precision and Accuracy of Results

To evaluate the precision and sensitivity of the four elements being determined, that is potassium, calcium, vanadium and chromium, thick targets of each of the four elements were analysed under bombardment with 3 MeV protons. The results obtained for thick targets are given in Table 4.1.

Table 4.1: Results of Analysis of Thick Targets

Element	Expected amount μg	Measured Counts/mCb	Found μg	Error	
				Absolute by mass	Relative %
Potassium	2.12	10 054	2.44	+0.32	+14.92
		8 843	2.38	+0.26	+12.45
		8 393	2.27	+0.15	+7.19
Calcium	1.50	23 612	1.70	+0.20	+13.10
		18 505	1.66	+0.16	+10.67
		19 286	1.93	+0.43	+28.82
Vanadium	0.506	84 563	0.469	-0.037	-7.26
		79 449	0.483	-0.023	-4.47
Chromium	0.420	61 191	0.447	+0.027	+6.39
		55 657	0.461	+0.041	+9.80

The expected amount (μg) corresponds to the mass of the element contained in 20μl pipetted on the pellet. The measured counts refer to the nett integrated count under the peak, calculated for a bombarding current of one millicoulomb.

The relative % error is *rather* high, but *unacceptably* high for potassium-calcium. A possible cause for the large discrepancies may be chromatographic separation of the elements in solution that could occur during the diffusion of the pipetted volume onto the urea matrix. From the analytical results it appears that chromatographic separation is more severe for the element pair potassium-calcium than for vanadium-chromium.

The expected amounts (μg) for thin targets were calculated from the yields and the amount obtained for thick targets using equation 1.6. Table 4.2 lists the results obtained for thin targets.

The overall relative error for thin targets is better than that for thick targets. One possible explanation is the fact that the intensity of the background is very much lower.

During the analysis of the adjacent elements, both the sensitivity and precision were evaluated by comparing the *experimentally* found mass concentration ratios with the *expected* ratios. An assessment of the results obtained for the analysis of the adjacent elements in thin targets are shown in Tables 4.3 and 4.4, where the measured values are the means of a set of similar analyses. Full details of the analysis are listed in Appendix B.2.

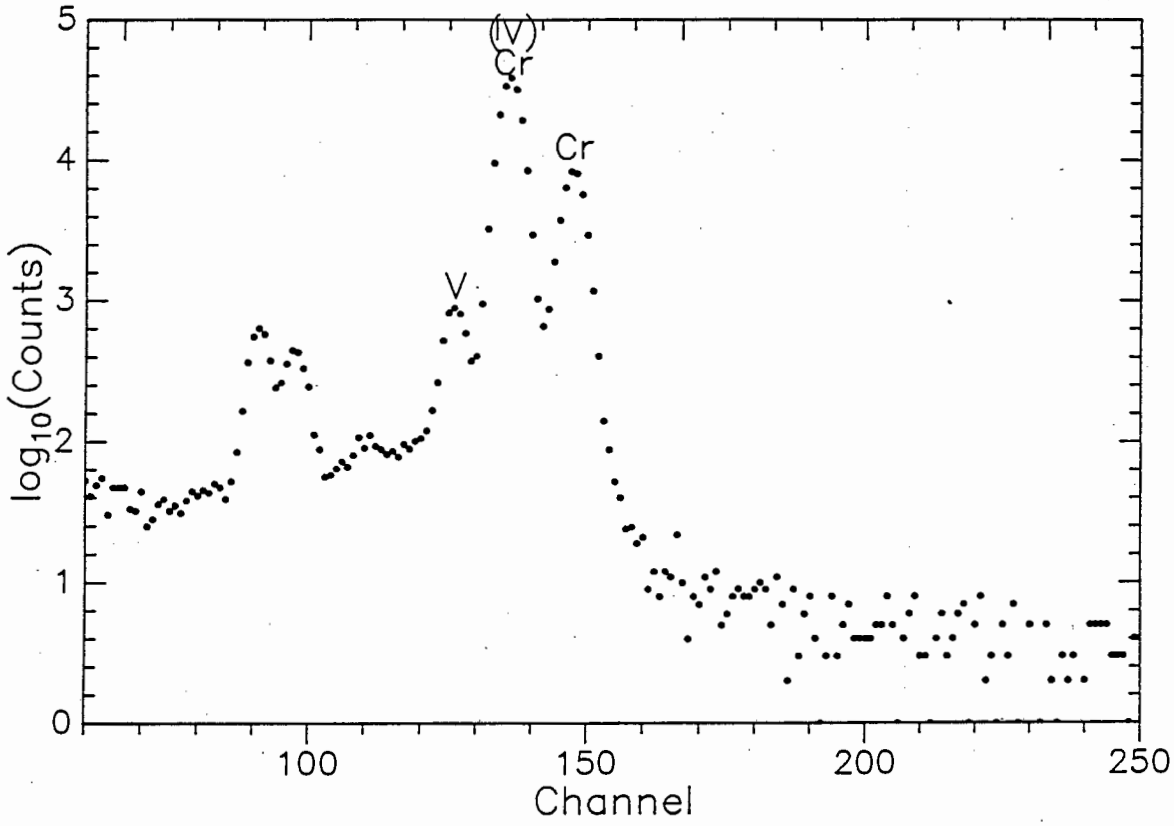

Figure 4.4: Energy spectrum of X-rays from a sample containing a high concentration of chromium.

Table 4.2: Results of Analysis of Thin Targets

Element	Expected amount μg	Measured Counts/mCb	Found μg	Error	
				Absolute by mass	Relative %
Potassium	1.44	103 053	1.42	-0.02	-1.60
		104 307	1.41	-0.03	-1.94
		95 566	1.48	+0.04	+2.89
		102 696	1.38	-0.06	-3.85
		105 047	1.48	+0.04	+2.89
Calcium	1.91	67 522	1.99	+0.08	+4.19
		68 333	1.95	+0.04	+2.09
		66 075	1.97	+0.06	+3.62
		62 543	1.89	-0.02	-1.14
Vanadium	0.529	130 897	0.509	-0.02	-3.78
		132 490	0.543	+0.014	+2.65
		141 338	0.540	+0.011	+2.08
Chromium	0.465	142 157	0.442	-0.023	-4.95
		141 026	0.448	-0.017	-3.66
		141 857	0.454	-0.011	-2.47
		139 396	0.446	-0.019	-4.09

Table 4.3: Determination of the adjacent elements

Potassium/Calcium pair Determination of Ca K_α				Calcium/Potassium pair Determination of K K_α			
Expected ratio by mass	Found ratio by mass	Difference Absolute by mass	Difference Relative %	Expected ratio by mass	Found ratio by mass	Difference Absolute by mass	Difference Relative %
10.12	10.5	+0.38	+3.75	9.90	11.22	+1.32	+13.33
20.28	18.8	-1.48	-7.3	19.84	22.36	+2.52	+12.7
50.0	49.27	-0.73	-1.46	48.78	49.19	+0.41	+0.84
97.09	99.53	+2.44	+2.51	96.15	101.87	+5.72	+5.95
197.24	199.25	+2.01	+1.02	198.41	207.58	+9.17	+4.62
505.1	184.66	-320.4	-63.4	500.1	209.55	-290.6	58.1
1010	180.7	-829.3	-82.1	961.5	191.4	-770.1	-80.1
4762	187.5	-4574.5	-96.1	5155	201.6	-4953.4	-96.1
9009	192.1	-8816.9	-97.9	9174	198.3	-8975.7	-97.8

By comparison, the results obtained for vanadium-chromium pair are better than those for potassium-calcium pair. This happens mainly because the peaks of both potassium and calcium lie near the maximum intensity of the bremsstrahlung background. Even if both elements were are present in a reasonably high concentration, the data were measured with a higher statistical error. The reverse is true for vanadium-chromium pair.

It is interesting to note that in both elemental pairs, a high concentration of element (Z+1) result in a significantly high yield of element Z X-rays, producing higher ratios. This happens because the *weak* K_β peak of element Z is being interfered by the more *intense* K_α peak of element (Z+1).

As expected, in both elemental pairs, the precision deteriorated as the concentration of the minor component decreased, because of increased errors of a statistical nature inherent in low count rates.

Although the AXIL program provided the areas of the interfering peaks separately, (i.e K_β of element Z and K_α of element Z+1), it fitted them as one peak. The degree to which the K_α peak of element Z+1 is being interfered with would therefore depend on the concentration of element Z. Thus the stripping of the spectrum is based on the assumption that the AXIL program can clearly distinguish between the two peaks. The error involved in the resolution of interfering lines can be deduced from the *chi-squared* value included in the print-out of an AXIL analysis. An example of an AXIL print-out is shown in Appendix A.

4.3 Determination of the adjacent elements

The program AXIL (see section 1.4.3) was used to determine the concentration of each of the elements in the element pairs. Since the program draws on information from the library of energies, the fact that the detector resolution is insufficient to resolve all the K_α and K_β spectrum peaks does not affect the reliability of the computed concentrations. However, the first requirement is that the program should

be able to locate the position of the peak in the spectrum. As the concentration of the minor component is reduced, a stage is reached where the program no longer recognises the existence of peaks corresponding to the minor component, and would report the existence of only one element. However, there exists the facility to force the program to determine components of which the corresponding peaks are not readily observable. By forcing the program to report on the areas of the peaks from X-rays of both elements, a value may be obtained, based on the prevailing background levels. These values are unlikely to be accurate.

Composite figures of the X-ray energy spectra obtained from samples in which the major component is progressively increased in concentration relative to the minor component are shown in Figs 4.5 to 4.8, where the major components are potassium, calcium, vanadium and chromium respectively. It may be noted that the presence of the minor component can no longer be recognised visually when the relative concentration exceeds 200 : 1. Under these conditions the values given in Appendix B are those obtained from AXIL when *forced* conditions requiring the evaluation of peak areas from *two* elements are demanded.

Table 4.4: Determination of the adjacent elements

Vanadium/Chromium pair Determination of Cr K_α				Chromium/Vanadium pair Determination of V K_α			
Expected ratio by mass	Found ratio by mass	Difference Absolute by mass	Difference Relative %	Expected ratio by mass	Found ratio by mass	Difference Absolute by mass	Difference Relative %
9.9	9.89	-0.01	-0.101	10.0	9.8	-0.2	-2
19.53	19.93	+0.4	+2.05	20.0	21.64	+1.64	+8.2
54.95	53.9	-1.05	-1.91	50.0	53.63	+3.63	+7.3
101.63	103.11	+1.48	+1.46	100.0	99.93	-0.07	-0.07
204.5	201.03	-3.47	-1.70	200.0	206.6	+6.6	+3.3
480.77	217.59	-263.18	-54.75	473.9	486.5	+12.6	+12.66
952.38	241.1	-711.3	-74.68	1003	334.04	-669.0	-66.7
4761	237.6	-4524.3	-95.01	4484.3	378.8	-4105.5	-91.6
9090	290.3	-8800.6	-96.8	9003	452.6	-8550.4	-95.0

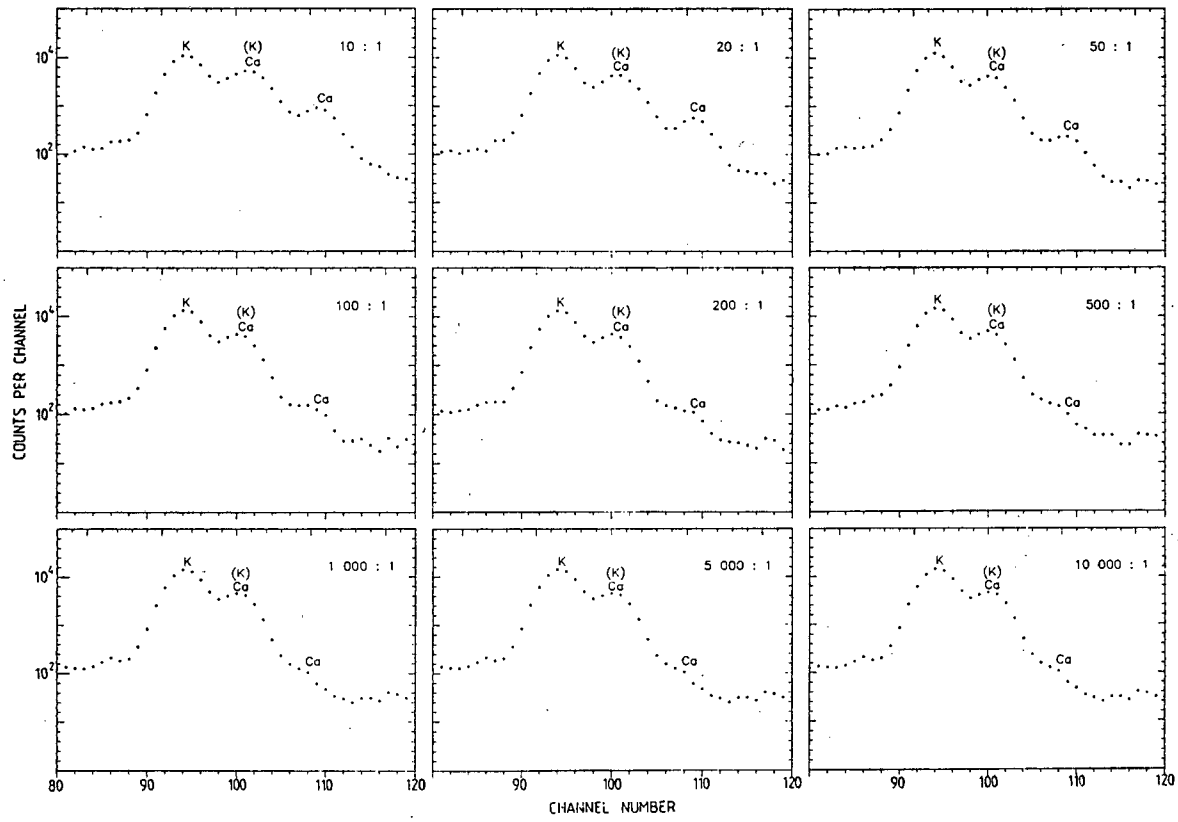

Figure 4.5: The X-ray energy spectra obtained from samples in which potassium is increased in concentration relative to calcium.

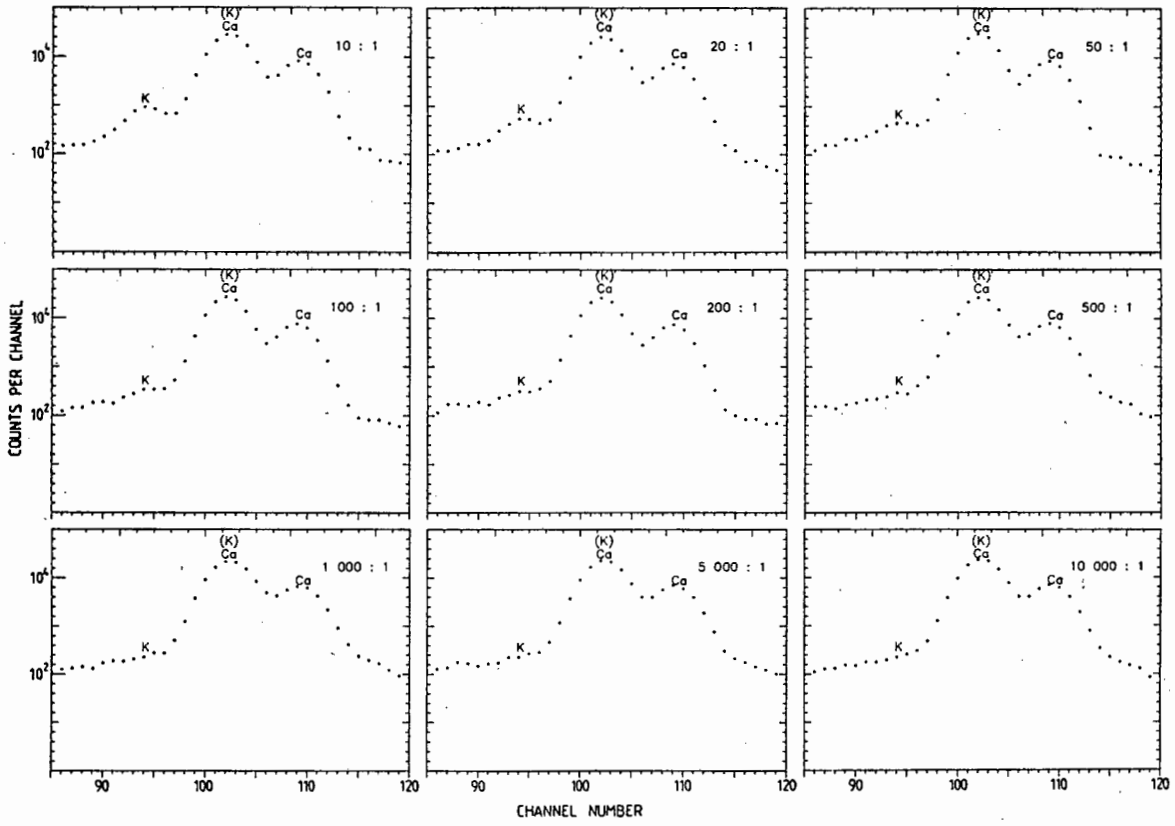

Figure 4.6: The X-ray energy spectra obtained from samples in which calcium is increased in concentration relative to potassium.

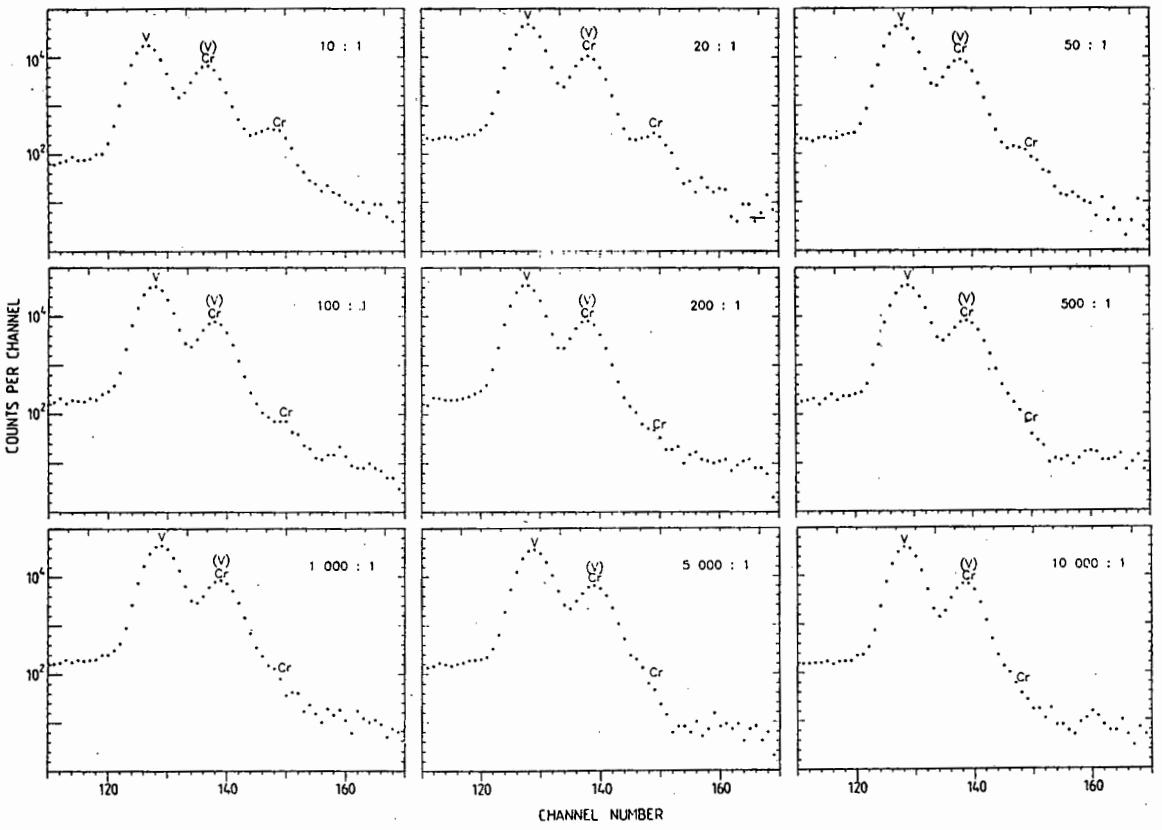

Figure 4.7: The X-ray energy spectra obtained from samples in which vanadium is increased in concentration relative to chromium.

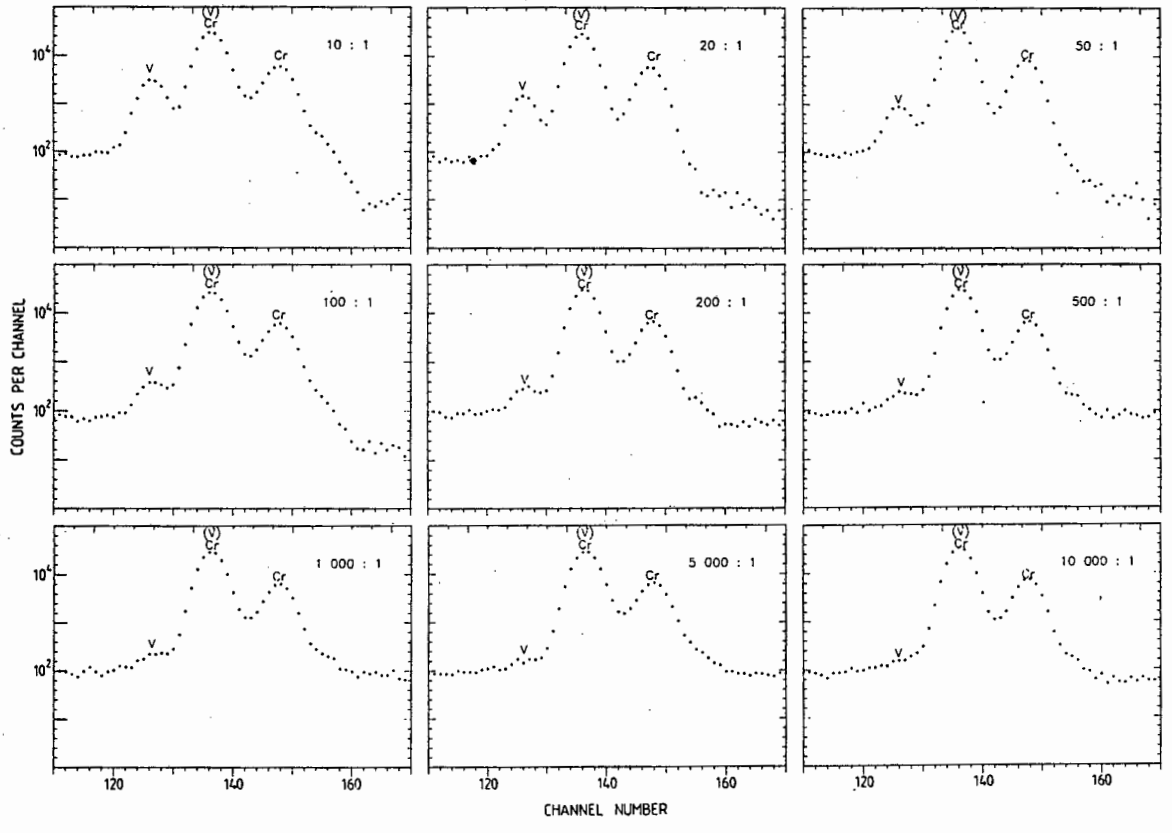

Figure 4.8: The X-ray energy spectra obtained from samples in which chromium is increased in concentration relative to vanadium.

4.4 Detection linearity

The experimentally determined concentration ratios were plotted against the known ratios. These plots are shown in Figs 4.9 to 4.16. Error bars represent the calculated relative precision from all the analysed samples of the same test solution, while the drawn line is that expected for ideal 1:1 correlation of the mean measured concentration to the known value. As long as the minor component yields sufficient X-rays to produce spectrum peaks which may be recognised by the program AXIL, the determined values are ratios calculated from the derived spectral peak areas. Deviation from linearity occurs when the minor component does not yield sufficient X-rays to form a recognizable peak in the spectrum. This happens when the concentration of the major component relative to that of the minor component exceeds 200 : 1 in all cases. It therefore represents the relative concentration limit for the detection of the minor component of adjacent elements.

When the major component exceeds 200 times that of the minor, the determined concentration ratio tends to a constant value. This value is an experimental artefact determined solely by the relative intensity of the background over the energy region where the X-rays of the minor component should have yielded a spectrum peak. Since all the spectra were measured under similar conditions, the spurious concentration ratio tends to a constant value.

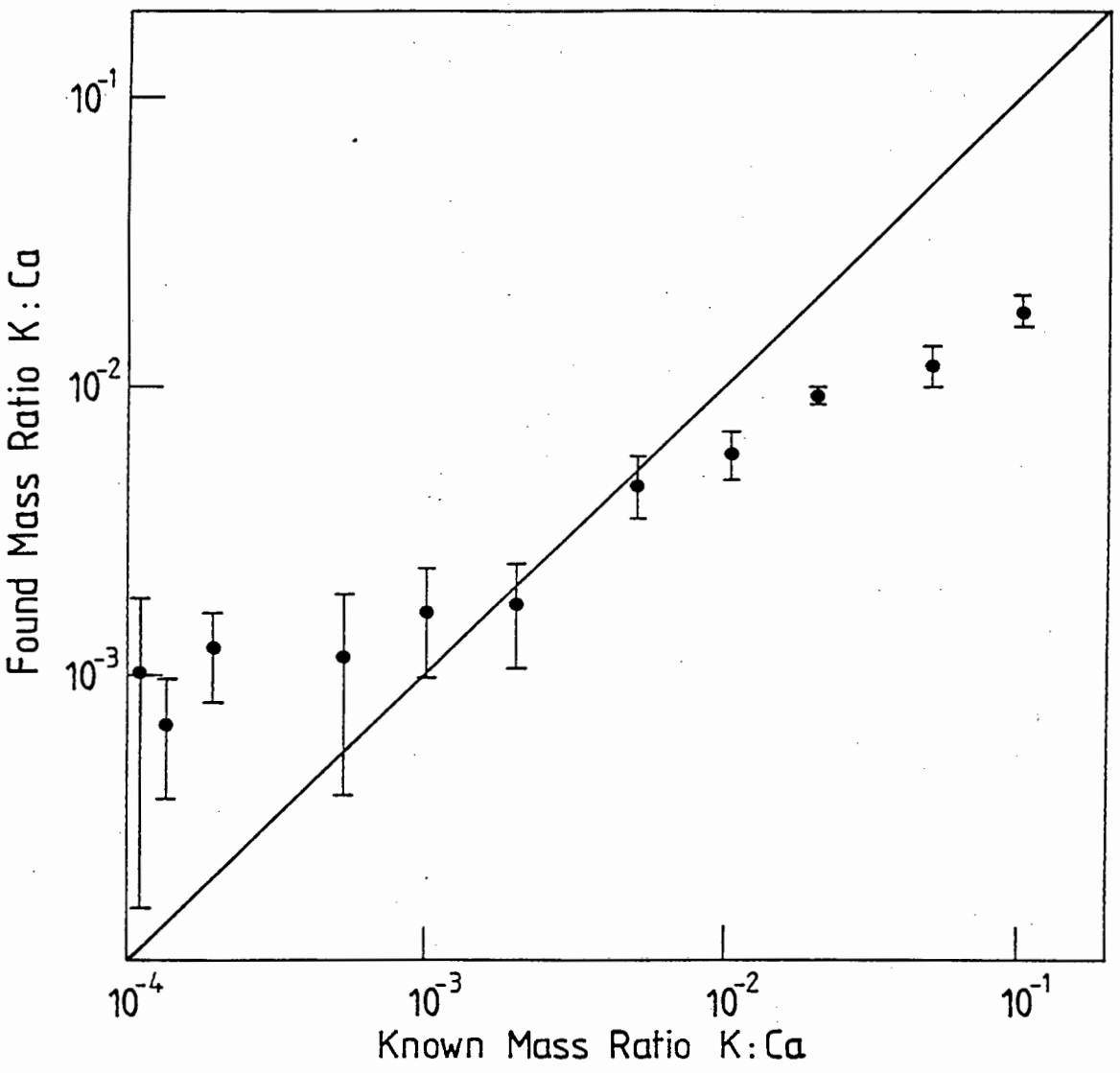

Figure 4.9: The experimentally determined concentration ratios against the known ratios for thick targets, K : Ca.

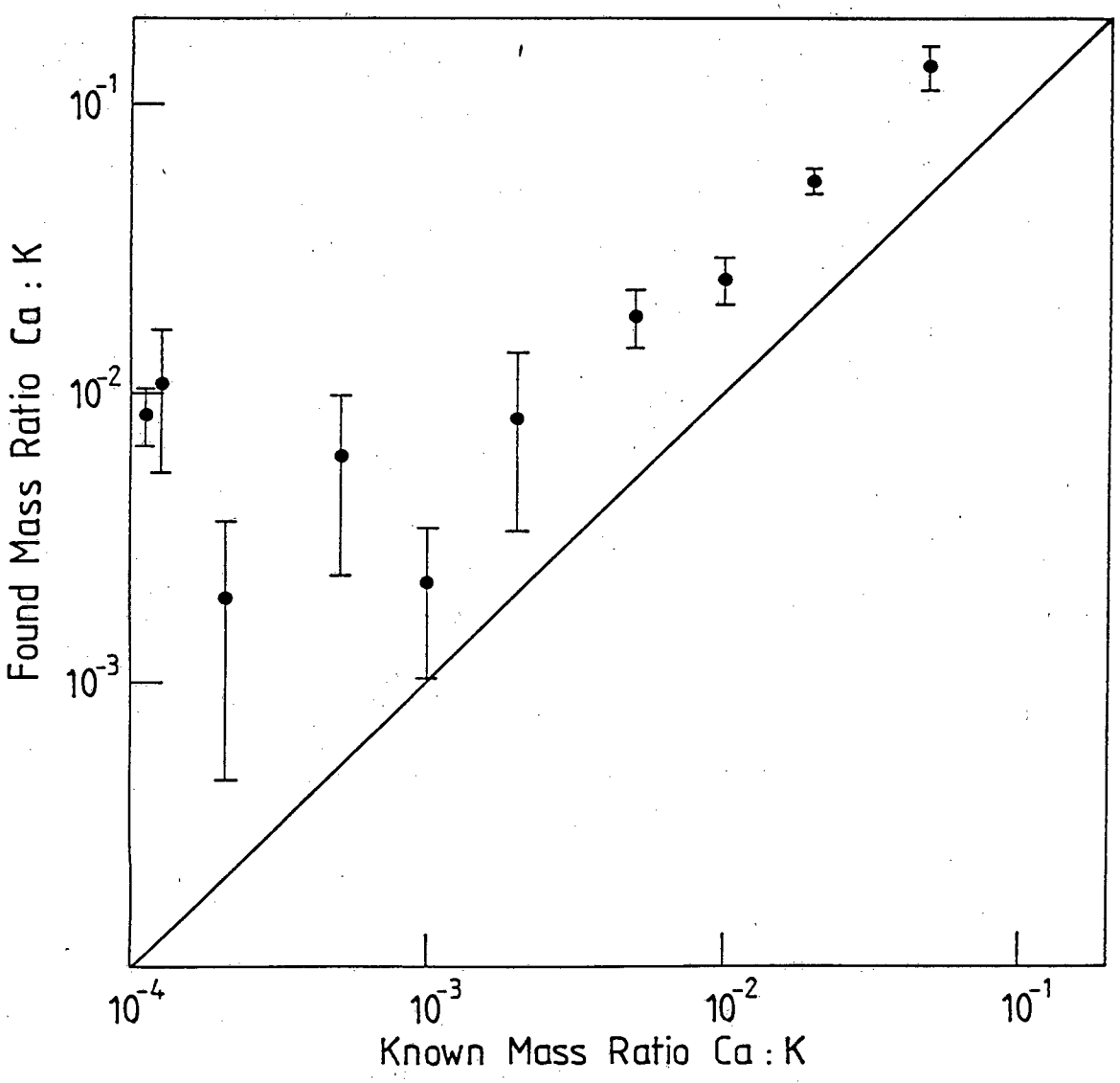

Figure 4.10: The experimentally determined concentration ratios against the known ratios for thick targets, Ca : K.

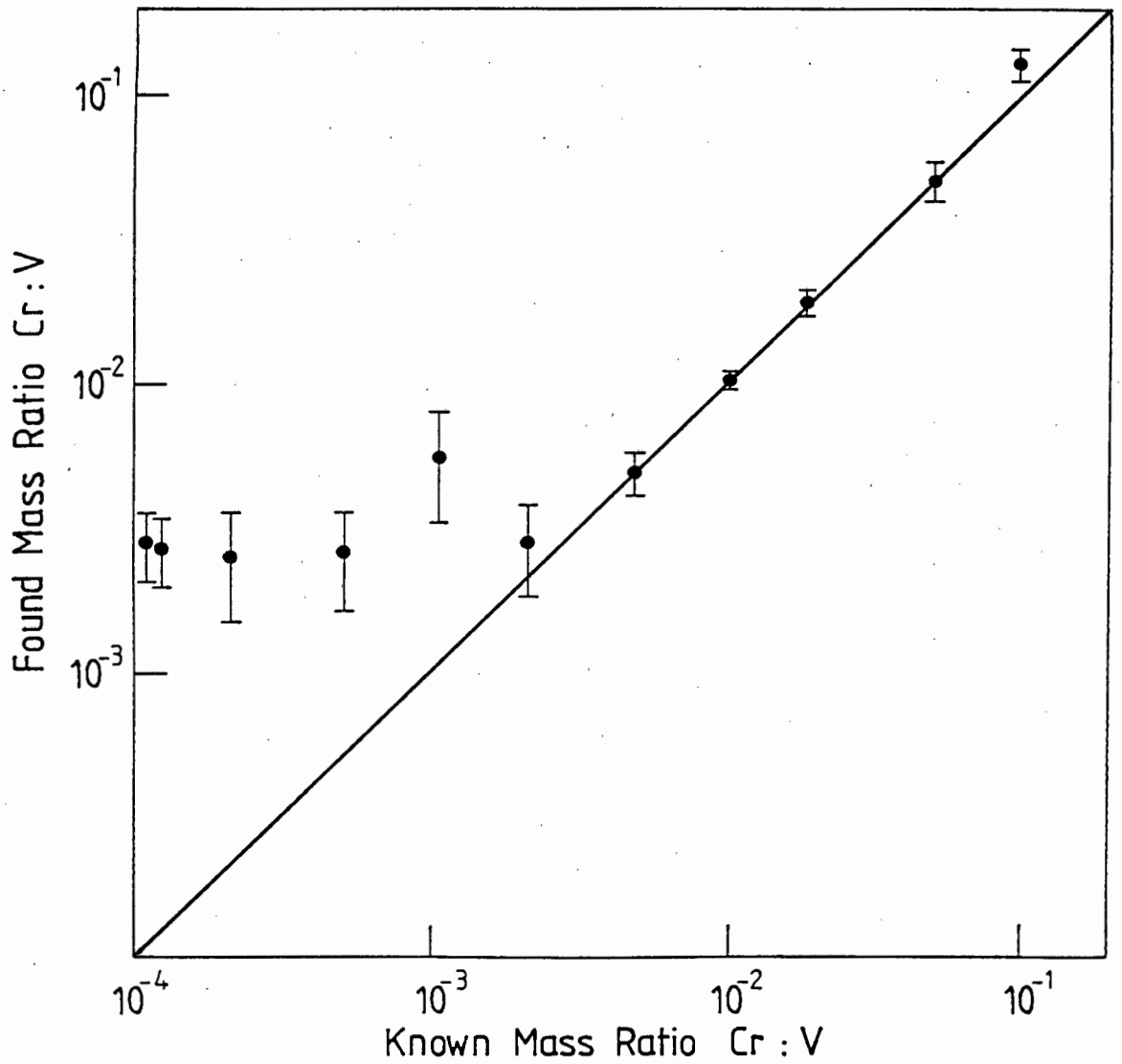

Figure 4.12: The experimentally determined concentration ratios against the known ratios for thick targets, Cr : V.

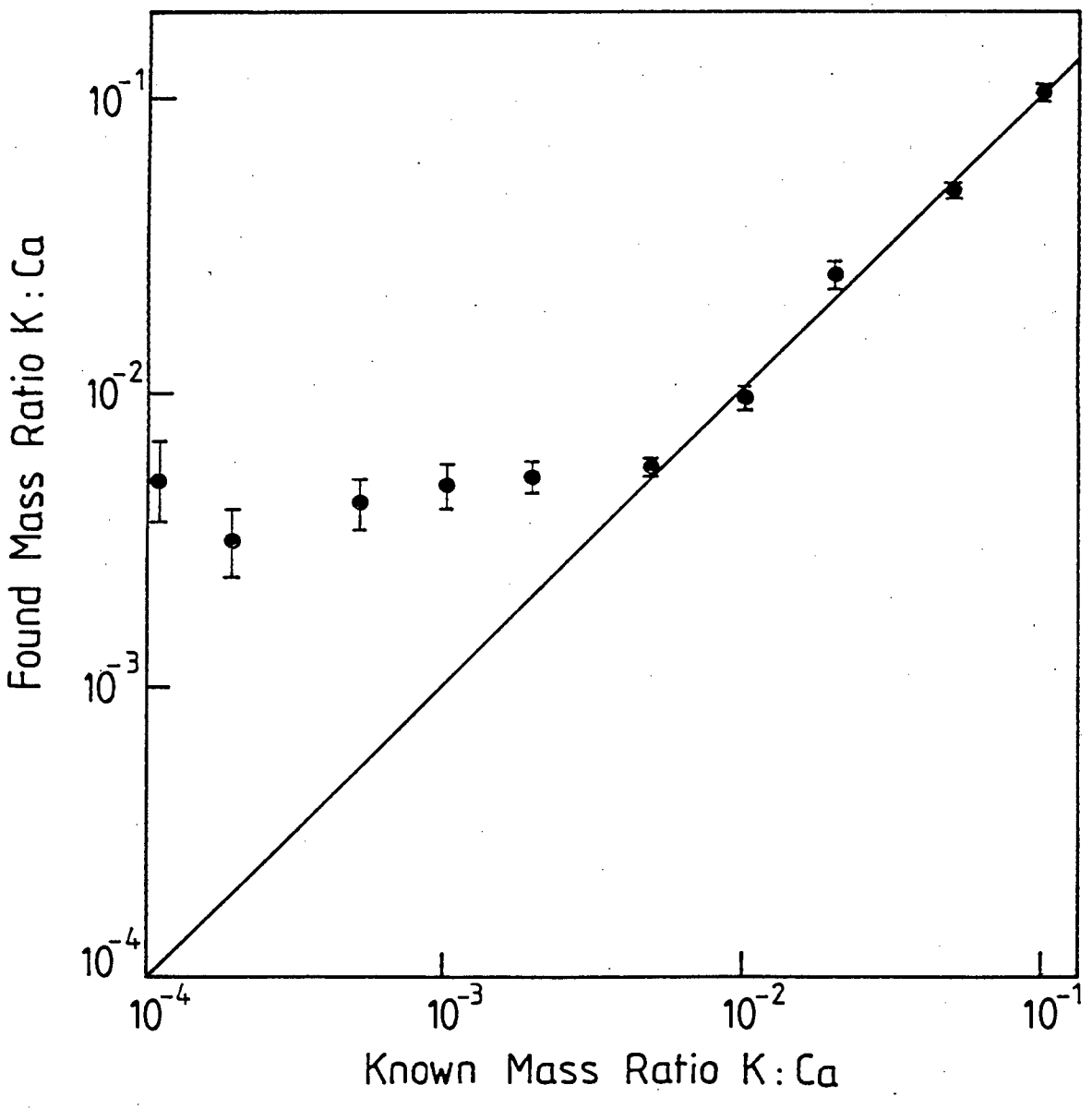

Figure 4.13: The experimentally determined concentration ratios against the known ratios for thin targets, K : Ca.

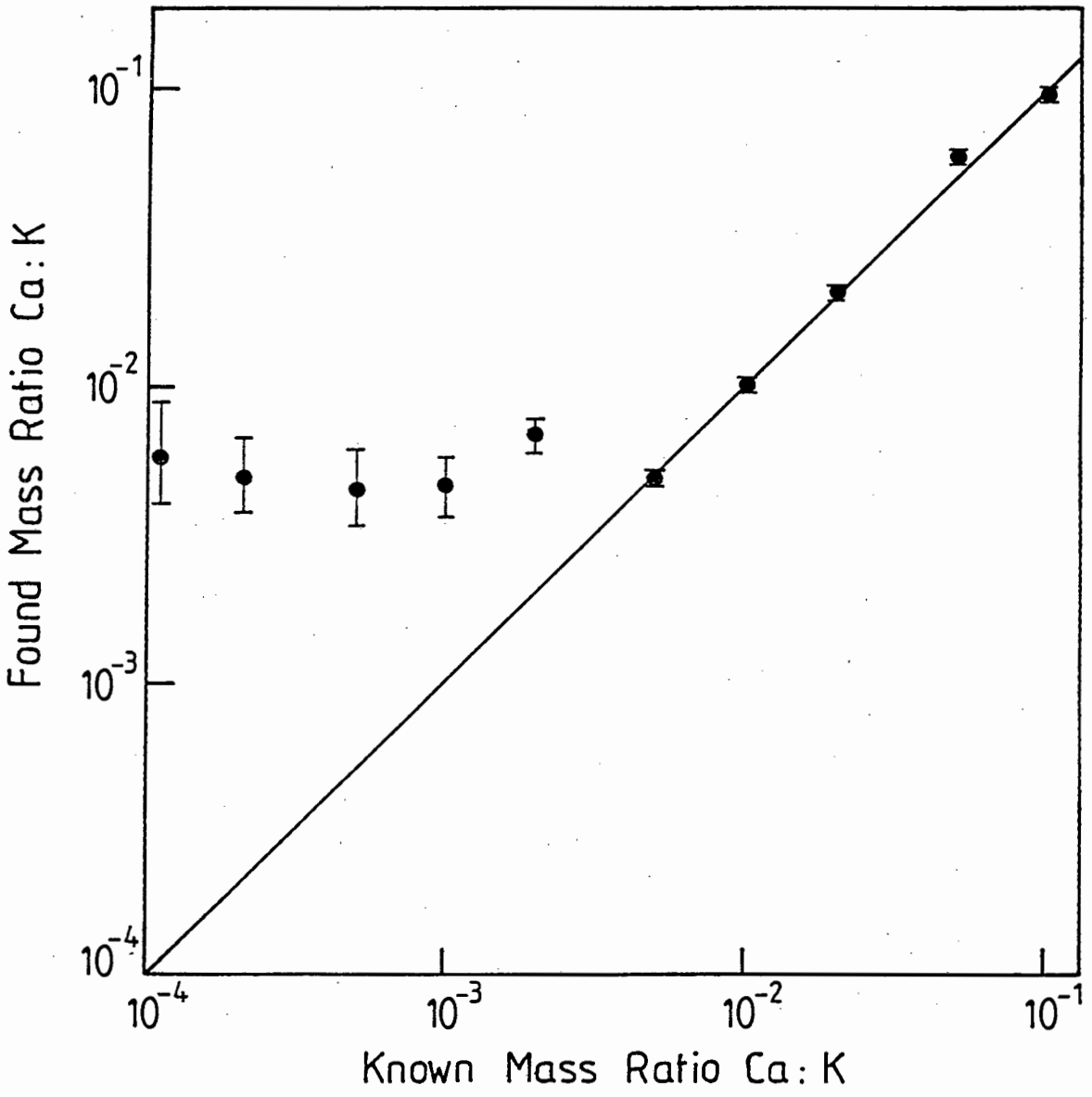

Figure 4.14: The experimentally determined concentration ratios against the known ratios for thin targets, Ca : K.

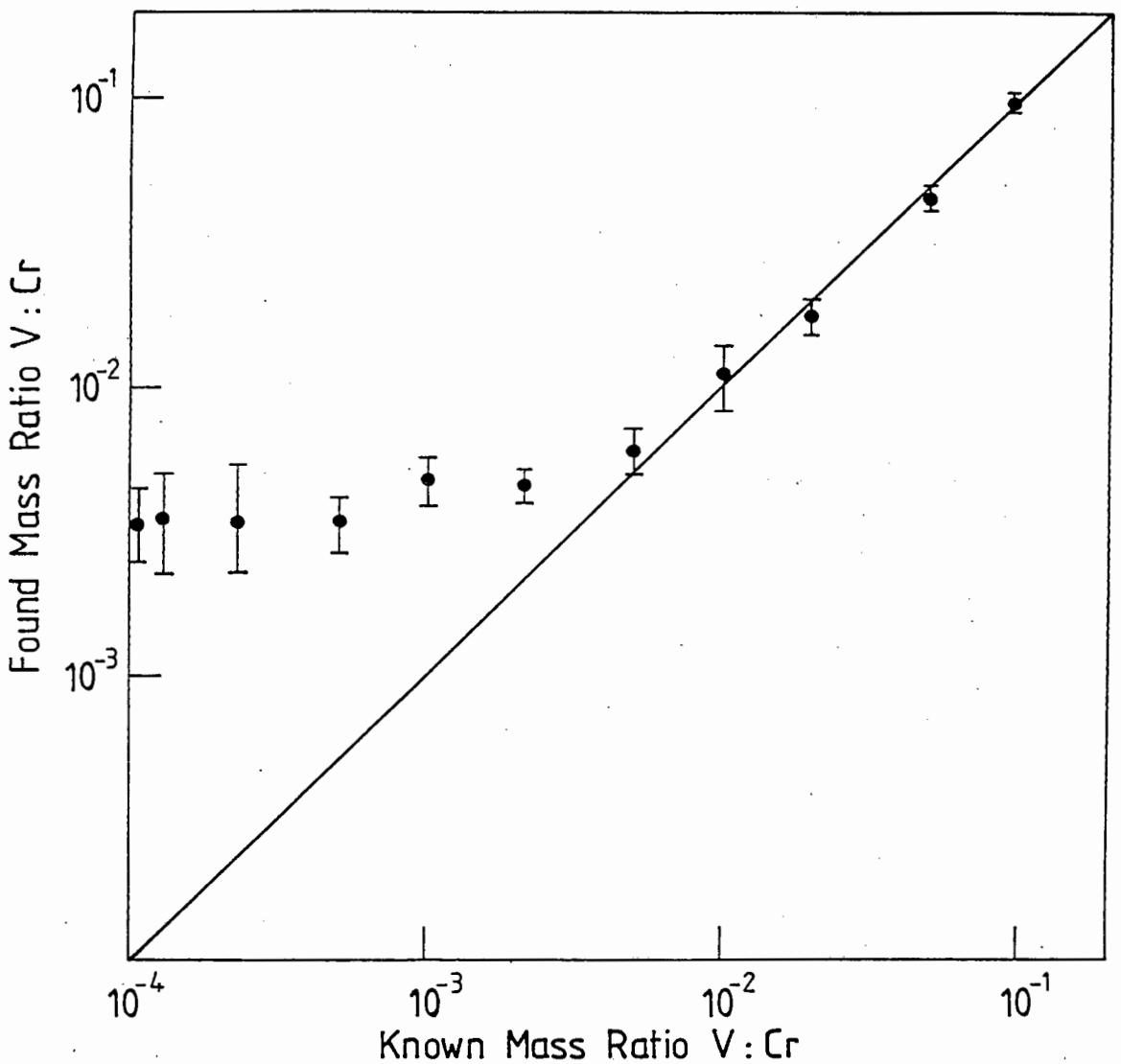

Figure 4.15: The experimentally determined concentration ratios against the known ratios for thin targets, V : Cr.

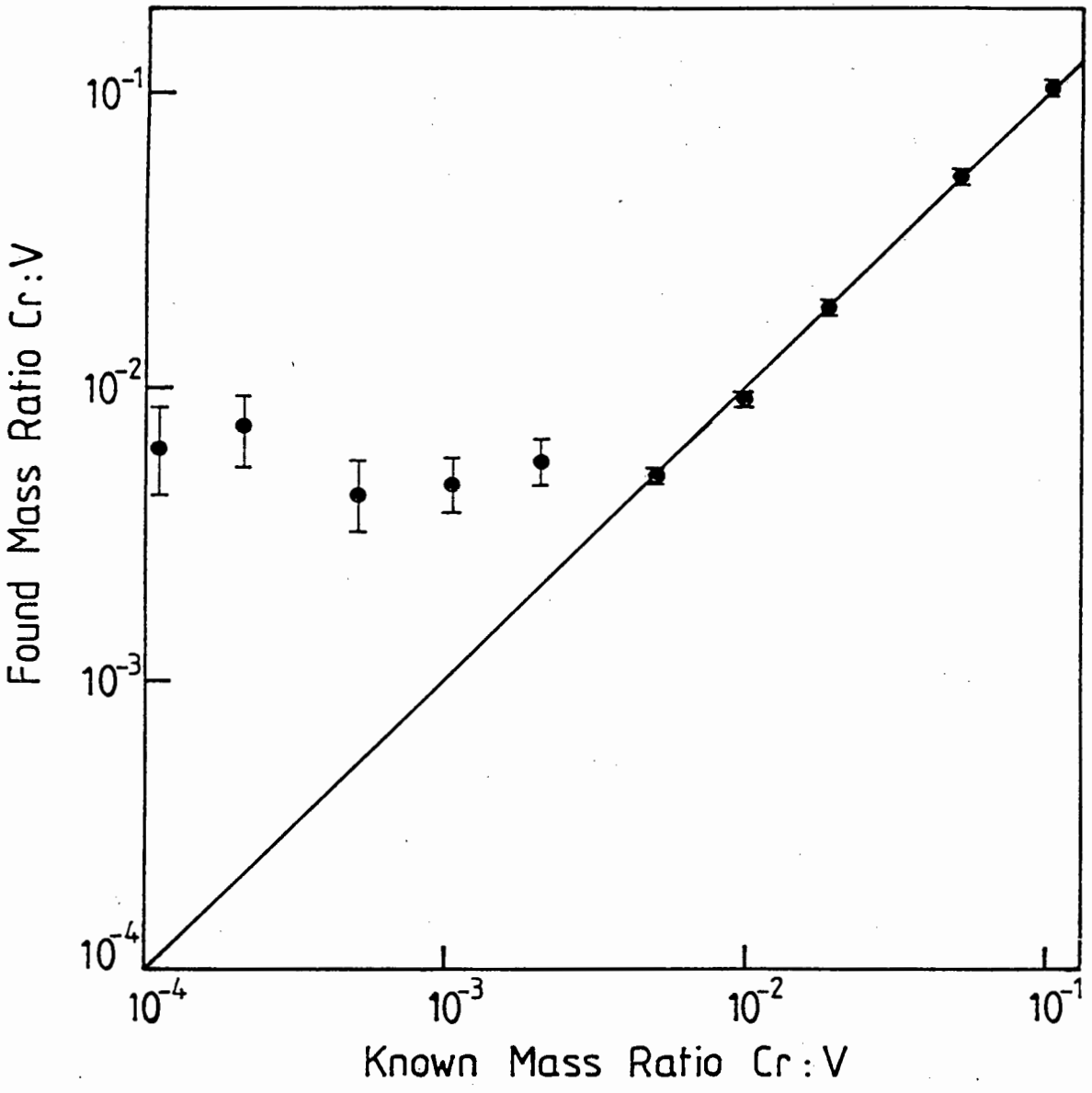

Figure 4.16: The experimentally determined concentration ratios against the known ratios for thin targets, Cr : V.

Despite the fact that the uniformity of thick targets containing the elemental pair V-Cr was poorer than thin targets of the same elements, the accuracy of the analysis of the tablets by X-ray spectrometry is good, as is shown by the proximity of the experimental points to the ideal correlation line in figures 4.11 and 4.12. Deviation from the ideal correlation line occurs at the same relative concentration as for thin targets. This implies that the chromatographic separation referred to previously (section 3.2) was a small effect which did not introduce unacceptably high errors.

The same cannot be said for the K-Ca case. The data represented in figures 4.9 and 4.10 clearly show that the experimental values fall far from the ideal correlation line. In figure 4.9 the test solutions containing relatively high concentrations of the minor component, potassium, gave results that lie *below* the expected values. This indicates that the bombarded spot on the target tablet yielded a lower intensity of K K_α X-rays due to the fact that the potassium salt diffuses more rapidly through the area matrix resulting in chromatographic separation and relative enrichment of calcium within the range of the bombarding protons. When the major component was potassium, diffusion of potassium again removed a portion of this component towards deeper depths within the area tablet, thus yielding relatively enriched calcium deposits, which produced experimental points *above* the expected values because the ratio that was plotted in figure 4.10 is the reciprocal of that plotted in figure 4.9.

Chapter 5

CONCLUSION

The study dealt with the determination of adjacent elements by PIXE when the peak of the K_β X-ray of the Z element overlapped that of the (Z+1) K_α X-ray in the X-ray energy spectrum measured by an energy dispersive intrinsic germanium detector. Two elemental pairs, potassium-calcium and vanadium-chromium were investigated. It was found that both elements in the pairs could be determined by PIXE accurately and with good precision as long as the relative concentration of the major component was less than 200 times that of the minor. This conclusion did not depend on which element in the pair was the major component, nor did the different elemental pairs yield different results. This conclusion was equally valid for thin and for thick samples.

It is, however, well-known that PIXE can achieve higher sensitivities on the high energy side of a high peak than on the low energy side. The reason high precision was not achieved arises from the need to handle *tailing* effects. The program AXIL does not have a mechanism to deal with tailing from the highest energy peak (produces higher background) on the low energy side of the spectrum, making the fitting of data points unreliable. However, on the high energy side of the large peak there is no tail, and AXIL fits the points well, (giving accurate peak areas). This can be seen in Tables 4.3 and 4.4 respectively.

Because of the difficulties involved in target preparation, the precision of the results from thin targets was better than those from thick. The preparation of thin targets involved the evaporation of droplets, of a solution containing both

elements, on an inert thin film of mylar. Thick targets were obtained by depositing similar solutions onto pellets of urea. Chromatographic separation of potassium and calcium in the urea pellets resulted in inhomogeneous thick samples which gave unsatisfactory analytical results, but the effect was not observed in vanadium-chromium samples. This is probably due to less separation between the latter samples and the higher X-ray energies of vanadium and chromium showing less absorption effects.

The program software, for deconvoluting measured spectra, plays a crucial role in determining the practical limit for analysing elemental pairs with overlapping spectrum peaks. The program AXIL could be *forced* to report on the presence of elements even when the software could not detect the necessary spectrum peaks.. Accordingly, under *forced* conditions, AXIL reported spurious concentrations of the minor component for relative concentration ratios greater than 200 : 1, depending on the intensities of the backgrounds in the energy region of the spectrum where the *forced* component was expected.

When the experimentally determined concentration of the minor element was plotted against its known concentration, deviation from linearity marked practical limit for analysis. This limit was a concentration ratio of 200 : 1, which was significantly dependent on the energy resolution of the detector, given by the full width at half the maximum height, of the order of 150 eV.

The results are of general validity when the intensity of the peak of element (Z+1) is less than that of element Z. However, if a small peak (element Z), is situated on the tail of a large peak, then the results are significantly dependent on the particular type of X-ray detector. The problem of tailing is most pronounced for the lighter elements (K, Ca), as the percentage of tailing increases for the lower X-ray energies. In addition it has not been possible to use a program with a correct response function, i.e. tailing is not well dealt with in the fitting.

REFERENCES

[Ak 74] R. Akselsson and T.B. Johansson, *Z. Physik,* 266, (1974) 245

[Al 25] S.K. Allison and W. Duane, *Proc. Nat. Sci.,* 11, (1925) 485

[Ba 11] C.G. Barkla, *Phil. Mag.,* 22, (1911) 396

[Bi 64] L.S. Birks and A.P. Batt, *Proceedings 14th Annual Symposium on Spectroscopy,* 111 (1964) 24

[Ca 86] J.L. Campbell, W. Maenhaut, E. Bombelka, E. Clayton, K. Malmqvist, J.A. Maxwell, J. Pallon and J. Vandenhaute, *Nucl. Instr. and Meth.,* B14 (1986) 204

[Cl 83] E. Clayton, *Nucl. Instr. and Meth.,* 218 (1983) 221

[Co 25] D. Coster and J. Nishina, *J. Chem. News,* 130 (1925) 149

[Cu 68] L.A. Currie, *Anal. Chem.,* 40 (1968) 586

[Fo 74] F. Folkmann, C. Gaarde, J. Huus and K. Kemp, *Nucl. Instr. and Meth.,* 116, (1974) 487

[Gi 76] I.S. Giles and M. Peisach, *J. Radioanal. Chem.,* 32, (1976) 105

[Gi 80] Gilson, *Instruction Manual,* "Pipetman", (1980)

[Gi 84] D. Gihwala, L. Jacobson, M. Peisach and C.A. Pineda, *Nucl. Instr. and Meth.,* B3 (1984) 408

[Ha 77] I. Hasselmann, W. Koenig, F.W. Richter, U. Steiner, U. Wätjen, C. Bode and W. Ohta, *Nucl. Instr. and Meth.,* 142 (1977) 163

[Is 76] K. Ishii and S. Morita, *Phys. Rev.,* A13, (1976) 131

[Jo 70] T.B. Johansson, R. Akselsson and S.A.E. Johansson, *Nucl. Instr. and Meth.,* 84 (1970) 141

[Jo 72] T.B. Johansson, R. Akselsson and S.A.E. Johansson, *Advan. X-ray Anal.,* 15 (1972) 373

[Jo 82] G.I. Johansson, *X-ray Spectrometry,* 11 (1982) 194

[Jo 88] S.A.E. Johansson and J.L. Campbell, *A novel technique for elemental analysis,* John Wiley and Sons, (1988) pg 158

[Ka 77] H.C. Kaufmann, R.K. Akselson and W.J Courtnay, *Nucl. Instr. and Meth.,* 142 (1977) 251

[Ma 63] D.W. Marquardt, *J. Soc. Ind. Appl. Math.,* 11 (1963) 431

[Ma 84] J.A. Maxwell, R.G. Leigh, J.L. Campbell and H. Paul, *Nucl. Instr. and Meth.,* B3 (1984) 301

[Me 69] E. Merzbacher, G.S. Khandelwal and B.H. Choi, *Atomic Data.* 1 (1969) 103

[Me 80] B.R. Meyer, *Application of proton-induced X-ray emission to a multi-element study of bitter pit in apples,* Thesis, University of Stellenbosch (1980)

[Mo 13] H.G.J. Moseley, em/Phil. Mag., 27 (1913) 703

[Pe 77] M. Peisach, B.R. Meyer and I.J. Van Heerden, em/Southern Universities Nuclear Institute Report, SUNI, 47 (1977)

[Pi 91] C.A. Pineda, *Elemental Analysis by Particle Accelerators,* (eds., B.Z Alfass and M. Peisach) CRS Press, Boca Ratron, USA, (in press)

[Qu 72] P. Quittner, *Gamma-ray spectroscopy,* Halsted Press, (1972)

[Re 80] M.J. Renan, *X-ray Spec.,* 9, (1980) 90

[Ro 69] J.T. Routt, and S.G. Prussin, *Nucl. Instr. and Meth.,* 72 (1969) 125

[Sa 74] S.I. Salem, S.L. Panossian and R.A. Krause, *Atomic Data and Nuclear Data Tables,* 14 (1974) 91

[Sc 74] J.H. Scofield, *Phys. Rev.,* A9 (1974) 1041

[St 76] P.J. Statham, *J. Phys.,* E9 (1976) 1023

[Va 77] P. Van Espen, H. Nullens and F. Adams, *Nucl. Instr. and Meth.,* 145 (1977) 579

[Va 77a] P. Van Espen, H. Nullens and F. Adams, *Nucl. Instr. and Meth.*, 142 (1977) 243

[Vo 32] G. Von Hevesey, *Chemical Analysis by X-ray and its applications*, McGraw-Hill, New York, (1932)

[Yo 73] F.C. Young, M.L. Roush and P.G. Breman, *Int. J. Appl. Radiat. Isot.*, 24 (1973) 153

APPENDIX A

A. AXIL output file

```
SPECTRUM   2985          AXIL VERS VAX      6-SEP-91  14:46:04
-------------------------------------------------------------
MCA COLLECT TIME    563. SEC

SYST  PIXI     MODE  0

REGI      70  -  140   /1    E0=   3.313

CTRL  CHISQR=  6.917  LCHANG= 6.37E-01 %  LAMDA=1.E-05     0 &19 ITER   12.6 SEC

BACK  LIN    B0  6.148E+01    B1 -6.964E+01
      QRE    B0  3.113E-03    B1 -5.239E-01    B2 -4.839E+00    B3  3.914E+00    B4 -8.415E-01

ABSO  DET    A1  4.699E-03    B1  4.840E-05    A2  7.580E-05    B2  6.990E-01
      FIL    A4  6.900E+01    B4 -2.853E+00

CALI  ENE   !C1   23.834     !C2   21.254     *C3  0.00000E+   *C4  0.00000E+0
      RES   C5   1.6783      C6  0.26997

ELEM     E,KEV       R        CHAN     FWHM      AREA        STDEV    CHI        TOTABS

K        3.313     89.638     94.2     178.      2322. +/-   112.    0.6       8.296E-02
         3.590     10.362    100.1     180.       443. +/-    21.    0.7       1.368E-01

CA       3.691     83.333    102.3     181.    113757. +/-   345.    0.8       1.591E-01
         4.013     16.667    109.1     184.     33555. +/-   102.    1.8       2.346E-01


SPECTRUM   2985          AXIL VERS VAX      6-SEP-91  14:46:05
-------------------------------------------------------------

   DATA      FIT    D              O=DATA     +=FIT     :=BACKG     *=DATA=FIT     $=DATA=FIT=BACK

                              28.              111.              442.              1758.             6986.             27766.
                              II---------------I-----------------I-----------------I-----------------I-----------------I
   142.      141.   0.    70-I-                                  $
   153.      138.   1.       I                                  :O
   144.      134.   1.       I                                 :O
   132.      131.   0.       I                                 $
   122.      128.  -1.       I                                O:
   104.      125.  -2.    75-I-                              O :
   100.      121.  -2.       I                              O  :
   107.      118.  -1.       I                              O:
   116.      115.   0.       I                              $
    96.      112.  -2.       I                             O  :
   115.      109.   1.    80-I-                             :O
    94.      108.  -1.       I                             O :
   136.      107.   2.       I                              :  O
   117.      106.   1.       I                              :O
   151.      112.   3.       I                              :   O
   157.      119.   3.    85-I-                             :  O
   145.      131.   1.       I                              :O
   150.      147.   0.       I                              $


   153.      169.  -1.       I                             O:
   179.      194.  -1.       I                               O:+
   225.      235.  -1.    90-I-                                :*
   312.      320.   0.       I                                :  O+
   477.      488.   0.       I                                :     *
   749.      722.   1.       I                                :        *
   901.      886.   0.       I                                :          *
   872.      851.  -1.    95-I-                               :           O+
   665.      679.  -1.       I                                :         O+
   674.      642.   1.       I                                :         +O
  1331.     1322.   0.       I                                :              *
  4111.     4124.   0.       I                                :                 *
 10871.    10903.   0.   100-I-                               :                    *
 20810.    20799.   0.       I                                :                      *
 27746.    27682.   1.       I                                 :                       *
 25765.    25507.   2.       I                                  :                       *
 16428.    16317.   1.       I                                   :                        *
  7583.     7582.   0.   105-I-                                  :                          *
  3781.     3681.   2.       I                                   :                      +O
  4134.     4180.  -1.       I                                    :                        *
  6589.     6641.  -1.       I                                     :                         *
  8110.     8200.  -1.       I                                      :                          *
  7002.     7165.  -2.   110-I-                                     :                           *
  4305.     4402.  -1.       I                                       :                         O+
  1881.     1929.  -1.       I                                        :                  O+
   590.      644.  -2.       I                                         :              O+
   215.      211.   0.       I                                          :         *
   131.      108.   2.   115-I-                                         : +  O
   125.       86.   3.       I                                          :   O
    75.       77.   0.       I                                           $
    71.       71.   0.       I                                            $
    66.       65.   0.       I                                             $
    39.       60.  -3.   120-I-   O                                        :
    46.       56.  -1.       I       O  :
    56.       52.   1.       I         :O
    54.       49.   1.       I        :O
    28.       46.  -3.       IO       :
    34.       44.  -2.   125-I- O     :
    49.       43.   1.       I      : O
    52.       42.   1.       I      :  O
    40.       41.   1.       I      : O
    37.       41.  -1.       I     O:
    41.       42.   0.   130-I-    $
    37.       43.  -1.       I    O :
    31.       44.  -2.       I O    :
    39.       45.  -1.       I    O :
    52.       46.   1.       I       :O
    36.       47.  -2.   135-I-  O   :
    57.       47.   1.       I       :  O
    42.       47.  -1.       I     O :
    39.       46.  -1.       I    O  :
    40.       44.   1.       I      :O
    32.       40.  -1.   140-I-O    :
```

APPENDIX B

B.1 Thick targets

B.1.1 The element pair potassium-calcium

B.1.1.1 Potassium as major component

The mean elemental ratio is given by $\overline{R} \times \frac{\sigma_{Ca}}{\sigma_K} = \overline{R} \times 0.87416$ and the relative precision is derived from the standard deviation of $\overline{R}$

Nominal elemental ratio								
K:Ca (10:1)			K:Ca (20:1)			K:Ca (50:1)		
Y(K)	Y(Ca)	Count ratio	Y(K)	Y(Ca)	Count ratio	Y(K)	Y(Ca)	Count ratio
49154	6239	7.88	44048	5550	7.94	47217	2373	19.90
43986	9262	4.75	44159	6164	7.16	48504	2509	19.33
34255	6995	4.90	49531	4549	10.89	52306	2114	24.74
43838	11118	3.94	50668	4979	10.18	49913	2291	21.79
45391	12161	3.73	48722	5592	8.71	47512	2147	22.13
$\overline{R}$ = mean count ratio = 5.04 Std. deviation ±1.66			$\overline{R}$ = mean count ratio = 8.98 Std. deviation ±1.54			$\overline{R}$ = mean count ratio = 21.58 Std. deviation ±2.13		
mean elemental ratio= 4.41 ± 1.45 (33.02%)			mean elemental ratio= 7.85 ± 1.35 (17.20%)			mean elemental ratio= 18.86 ± 1.86 (9.89%)		

B.1.1 The element pair potassium-calcium

B.1.1.1 Potassium as major component

The mean elemental ratio is given by $\overline{R} \times \frac{\sigma_{Ca}}{\sigma_K} = \overline{R} \times 0.87416$ and the relative precision is derived from the standard deviation of $\overline{R}$

Nominal elemental ratio								
K:Ca (100:1)			K:Ca (200:1)			K:Ca (500:1)		
Y(K)	Y(Ca)	Count ratio	Y(K)	Y(Ca)	Count ratio	Y(K)	Y(Ca) *(Forced)*	Count ratio
52372	1397	37.49	54231	678	79.99	58576	451	129.88
48007	1185	40.51	52928	946	55.95	60759	848	71.65
54739	1080	50.68	56590	1180	47.96	55893	435	128.49
47756	813	58.74	56581	702	80.60	56224	519	108.33
46537	860	54.11	55998	1157	48.40	56150	570	98.51
56663	1305	43.42	54720	699	78.28	42576	134	317.73
			52066	801	65.0	69297	190	364.72
$\overline{R}$ = mean count ratio = 47.49			$\overline{R}$ = mean count ratio = 65.17			$\overline{R}$ = mean count ratio = 174.19		
Std. deviation ±8.32			Std. deviation ±14.68			Std. deviation ±116.57		
mean elemental ratio= 41.51 ± 7.27 (17.51%)			mean elemental ratio= 56.97 ± 12.83 (22.52%)			mean elemental ratio= 152.27 ± 101.90 (66.92%)		

B.1.1 The element pair potassium-calcium

B.1.1.1 Potassium as major component

The mean elemental ratio is given by $\overline{R} \times \frac{\sigma_{Ca}}{\sigma_K} = \overline{R} \times 0.87416$ and the relative precision is derived from the standard deviation of $\overline{R}$

Nominal elemental ratio								
K:Ca (1 000:1)			K:Ca (5 000:1)			K:Ca (10 000:1)		
Y(K)	Y(Ca) *(Forced)*	Count ratio	Y(K)	Y(Ca) *(Forced)*	Count ratio	Y(K)	Y(Ca) *(Forced)*	Count ratio
62655	59	1062	58753	145	405.2	77047	609	126.5
62754	168	373.5	57777	209	276.4	80979	706	114.7
59702	201	297.0	58334	29	2011	70583	404	174.7
52881	55	961.5	60009	286	209.8	83299	785	106.1
61647	107	576.1	52000	27	1926	74339	521	142.7
74345	402	184.9	63127	71	889.1	74375	417	178.4
$\overline{R}$ = mean count ratio = 575.8 Std. deviation ±362.3			$\overline{R}$ = mean count ratio = 952.9 Std. deviation ±822.2			$\overline{R}$ = mean count ratio = 140.5 Std. deviation ±30.5		
mean elemental ratio= 503.3 ± 316.7 (62.92%)			mean elemental ratio= 833.0 ± 718.7 (86.29%)			mean elemental ratio= 198.3 ± 140.5 (21.7%)		

B.1.1 The element pair calcium-potassium.

B.1.1.2 Calcium as major component

The mean elemental ratio is given by $\overline{R} \times \frac{\sigma_K}{\sigma_{Ca}} = \overline{R} \times 1.14396$ and the relative precision is derived from the standard deviation of $\overline{R}$

Nominal elemental ratio								
Ca:K (10:1)			Ca:K (20:1)			Ca:K (50:1)		
Y(Ca)	Y(K)	Count ratio	Y(Ca)	Y(K)	Count ratio	Y(Ca)	Y(K)	Count ratio
78203	1600	48.88	101101	1529	66.12	116007	1234	94.01
78137	1281	61.0	101536	1400	72.53	116751	1260	92.66
96996	2053	47.25	95773	1120	85.51	117592	1129	104.16
113329	2569	44.11	98797	1533	64.45	102947	1161	88.67
99989	2216	45.12	112256	1223	91.79	99767	1093	91.28
$\overline{R}$ = mean count ratio = 49.27 Std. deviation ±6.81			$\overline{R}$ = mean count ratio = 76.08 Std. deviation ±12.07			$\overline{R}$ = mean count ratio = 94.15 Std. deviation ±5.93		
mean elemental ratio= 56.36 ± 7.79 (13.82%)			mean elemental ratio= 87.03 ± 13.81 (15.87%)			mean elemental ratio= 107.7 ± 6.78 (6.30%)		

B.1.1 The element pair calcium-potassium.

B.1.1.2 Calcium as major component

The mean elemental ratio is given by $\overline{R} \times \frac{\sigma_K}{\sigma_{Ca}} = \overline{R} \times 1.14396$ and the relative precision is derived from the standard deviation of $\overline{R}$

Nominal elemental ratio								
Ca:K (100:1)			Ca:K (200:1)			Ca:K (500:1)		
Y(Ca)	Y(K)	Count ratio	Y(Ca)	Y(K)	Count ratio	Y(Ca)	Y(K) *(Forced)*	Count ratio
106271	784	135.55	122055	484	252.18	108924	235	463.51
116001	650	178.46	101138	468	216.11	107420	251	427.97
106713	925	115.37	98827	486	203.35	100554	112	897.8
91536	475	192.71	100364	630	159.31	118527	214	553.86
110628	785	140.93	111913	423	264.57	105124	136	772.97
100186	619	161.85	101772	617	164.95			
			105450	755	139.67			
$\overline{R}$ = mean count ratio = 154.14 Std. deviation ±28.85			$\overline{R}$ = mean count ratio = 200.02 Std. deviation ±47.76			$\overline{R}$ = mean count ratio = 623.22 Std. deviation ±203.9		
mean elemental ratio= 176.33 ± 33.0 (18.72%)			mean elemental ratio= 228.81 ± 54.64 (23.88%)			mean elemental ratio= 712.94 ± 233.2 (32.71%)		

B.1.1 The element pair calcium-potassium.

B.1.1.2 Calcium as major component

The mean elemental ratio is given by $\overline{R} \times \frac{\sigma_K}{\sigma_{Ca}} = \overline{R} \times 1.14396$ and the relative precision is derived from the standard deviation of $\overline{R}$

Nominal elemental ratio								
Ca:K (1 000:1)			Ca:K (5 000:1)			Ca:K (10 000:1)		
Y(Ca)	Y(K) *(Forced)*	Count ratio	Y(Ca)	Y(K) *(Forced)*	Count ratio	Y(Ca)	Y(K) *(Forced)*	Count ratio
104695	254	412.2	96401	132	730.3	98829	40	2470
107832	187	576.6	92747	86	1079.	108893	41	2656
111071	129	861.0	87336	193	452.5	106242	102	1042
106499	121	880.2	97373	115	846.7	100200	304	329.6
107687	358	300.8	96518	39	2475	106397	222	479.3
99827	135	739.5	41425	54	767.1	105098	165	637.0
93761	249	376.6				99060	28	3538
$\overline{R}$ = mean count ratio = 592.4			$\overline{R}$ = mean count ratio = 1058.3			$\overline{R}$ = mean count ratio = 1593.1		
Std. deviation ±238.4			Std. deviation ±722.6			Std. deviation ±1273.9		
mean elemental ratio= 677.7 ± 272.7 (40.24%)			mean elemental ratio= 1210.7 ± 826.6 (68.28%)			mean elemental ratio= 1822 ± 1457 (79.96%)		

B.1.2 The element pair vanadium-chromium

B.1.2.1 Vanadium as major component

The mean elemental ratio is given by $\overline{R} \times \frac{\sigma_{Cr}}{\sigma_V} = \overline{R} \times 0.84068$ and the relative precision is derived from the standard deviation of $\overline{R}$

Nominal elemental ratio								
V:Cr (10:1)			V:Cr (20:1)			V:Cr (50:1)		
Y(V)	Y(Cr)	Count ratio	Y(V)	Y(Cr)	Count ratio	Y(V)	Y(Cr)	Count ratio
80860	7055	11.46	236038	11374	20.75	198682	3066	64.80
83218	9185	9.06	208673	7184	29.05	221490	4052	54.66
84716	7923	10.69	219158	7951	27.56	204202	3711	55.03
79036	9400	8.408	233009	10819	21.54	210345	3078	68.34
88996	9644	9.228	205847	9205	22.36	202727	2967	68.33
						203446	2945	69.08
						200752	3250	61.77
$\overline{R}$ = mean count ratio = 9.77			$\overline{R}$ = mean count ratio = 24.25			$\overline{R}$ = mean count ratio = 63.14		
Std. deviation ±1.261			Std. deviation ±3.78			Std. deviation ±6.21		
mean elemental ratio= 8.213 ± 1.06 (12.91%)			mean elemental ratio= 20.39 ± 3.18 (15.58%)			mean elemental ratio= 53.08 ± 5.22 (9.84%)		

B.1.2 The element pair vanadium-chromium

B.1.2.1 Vanadium as major component

The mean elemental ratio is given by $\overline{R} \times \frac{\sigma_{Cr}}{\sigma_V} = \overline{R} \times 0.84068$ and the relative precision is derived from the standard deviation of $\overline{R}$

Nominal elemental ratio								
V:Cr (100:1)			V:Cr (200:1)			V:Cr (500:1)		
Y(V)	Y(Cr)	Count ratio	Y(V)	Y(Cr)	Count ratio	Y(V)	Y(Cr) *(Forced)*	Count ratio
185869	1579	117.71	205660	827	248.68	278253	370	752.04
198109	1793	110.49	252820	1178	214.62	255770	321	796.79
211428	1851	114.22	252125	1113	226.53	241500	533	453.1
209321	2154	97.18	237803	679	350.23	272727	427	638.7
231532	2442	94.81	270861	1303	207.87	248676	432	575.64
96944	808	119.98	230401	1019	226.11	224578	461	487.15
						208690	638	327.1
$\overline{R}$ = mean count ratio = 109.07 Std. deviation ±10.65			$\overline{R}$ = mean count ratio = 245.67 Std. deviation ±53.07			$\overline{R}$ = mean count ratio = 575.79 Std. deviation ±167.64		
mean elemental ratio= 91.69 ± 8.95 (9.76%)			mean elemental ratio= 206.53 ± 44.61 (21.60%)			mean elemental ratio= 484.06 ± 140.93 (29.11%)		

B.1.2 The element pair vanadium-chromium

B.1.2.1 Vanadium as major component

The mean elemental ratio is given by $\overline{R} \times \frac{\sigma_{Cr}}{\sigma_K} = \overline{R} \times 0.84068$ and the relative precision is derived from the standard deviation of $\overline{R}$

Nominal elemental ratio								
V:Cr (1 000:1)			V:Cr (5 000:1)			V:Cr (10 000:1)		
Y(V)	Y(Cr) *(Forced)*	Count ratio	Y(V)	Y(Cr) *(Forced)*	Count ratio	Y(V)	Y(Cr) *(Forced)*	Count ratio
232840	449	518.6	171743	230	746.7	175917	548	321.0
205236	546	375.9	185208	156	1187	166199	421	394.8
178877	607	294.7	180914	361	501.2	170315	550	309.7
209321	430	486.8	181582	394	460.9	170666	208	820.5
259102	750	345.5	185383	368	503.8	170298	434	392.4
208324	609	342.1	184193	465	396.1	177266	387	458.1
212998	369	577.2	182455	692	263.7	195470	452	432.5
			176126	462	381.2	179494	369	486.4
$\overline{R}$ = mean count ratio = 420.1 Std. deviation ±106.6			$\overline{R}$ = mean count ratio = 555.1 Std. deviation ±290.6			$\overline{R}$ = mean count ratio = 451.9 Std. deviation ±161.1		
mean elemental ratio= 353.1 ± 89.61 (25.37%)			mean elemental ratio= 466.7 ± 244.3 (52.35%)			mean elemental ratio= 379.9 ± 135.4 (35.65%)		

B.1.2 The element pair vanadium-chromium

B.1.1.2 Chromium as major component

The mean elemental ratio is given by $\overline{R} \times \frac{\sigma_V}{\sigma_{Cr}} = \overline{R} \times 1.18952$ and the relative precision is derived from the standard deviation of $\overline{R}$

Nominal elemental ratio								
Cr:V (10:1)			Cr:V (20:1)			Cr:V (50:1)		
Y(Cr)	Y(V)	Count ratio	Y(Cr)	Y(V)	Count ratio	Y(Cr)	Y(V)	Count ratio
137531	15045	9.14	143854	8170	17.61	59981	1098	54.63
135438	13782	9.83	131988	8371	15.77	65096	1317	49.43
137863	16194	8.51	144389	9262	14.79	63291	1056	59.93
124972	14872	8.40	125607	9481	13.25	58785	1259	46.69
125465	14668	8.55	142011	7411	19.16	73264	1448	50.60
$\overline{R}$ = mean count ratio = 8.89 Std. deviation ±0.60			$\overline{R}$ = mean count ratio = 16.12 Std. deviation ±2.32			$\overline{R}$ = mean count ratio = 52.26 Std. deviation ±5.15		
mean elemental ratio= 10.57 ± 0.71 (6.74%)			mean elemental ratio= 19.18 ± 2.76 (14.42%)			mean elemental ratio= 62.16 ± 6.13^{a} (9.86%)		

B.1.2 The element pair vanadium-chromium

B.1.2.2 Chromium as major component

The mean elemental ratio is given by $\overline{R} \times \frac{\sigma_V}{\sigma_{Cr}} = \overline{R} \times 1.18952$ and the relative precision is derived from the standard deviation of $\overline{R}$

Nominal elemental ratio								
Cr:V (100:1)			Cr:V (200:1)			Cr:V (500:1)		
Y(Cr)	Y(V)	Count ratio	Y(Cr)	Y(V)	Count ratio	Y(Cr)	Y(V) *(Forced)*	Count ratio
122101	1216	100.16	136159	792	171.92	130181	717	181.56
124078	1337	92.80	123125	896	137.42	131590	754	174.52
129953	1884	68.98	119064	716	166.29	132557	640	207.12
94833	789	120.19	124929	684	182.64	133143	693	192.13
126282	1552	81.37	124074	916	135.45	133180	816	163.21
			123845	899	137.76	132521	918	144.36
						135597	684	198.24
						131576	637	206.56
$\overline{R}$ = mean count ratio = 92.70 Std. deviation ±19.38			$\overline{R}$ = mean count ratio = 155.25 Std. deviation ±20.81			$\overline{R}$ = mean count ratio = 183.46 Std. deviation ±22.07		
mean elemental ratio= 110.27 ± 23.05 (20.91%)			mean elemental ratio= 184.67 ± 24.75 (13.41%)			mean elemental ratio= 218.23 ± 26.25 (12.03%)		

B.1.2 The element pair vanadium-chromium

B.1.2.2 Chromium as major component

The mean elemental ratio is given by $\overline{R} \times \frac{\sigma_V}{\sigma_{Cr}} = \overline{R} \times 1.18952$ and the relative precision is derived from the standard deviation of $\overline{R}$

Nominal elemental ratio								
Cr:V (1 000:1)			Cr:V (5 000:1)			Cr:V (10 000:1)		
Y(Cr)	Y(V) *(Forced)*	Count ratio	Y(Cr)	Y(V) *(Forced)*	Count ratio	Y(Cr)	Y(V) *(Forced)*	Count ratio
137165	692	198.2	139059	351	396.2	145708	550	264.9
141300	661	213.8	148860	654	227.6	133830	491	272.6
151342	829	182.6	127733	487	262.3	148562	424	350.4
162952	906	179.9	144421	578	249.9	135813	568	239.11
161213	881	182.99	142189	485	293.2	142856	618	231.2
118164	566	208.77	141492	636	222.5	157347	670	234.9
125270	636	197	138262	410	337.2	155678	550	283.1
			125824	522	241.0	153622	499	307.9
$\overline{R}$ = mean count ratio = 194.7			$\overline{R}$ = mean count ratio = 278.7			$\overline{R}$ = mean count ratio = 271.6		
Std. deviation ±13.44			Std. deviation ±60.62			Std. deviation ±43.99		
mean elemental ratio= 231.6 ± 15.99 (6.9%)			mean elemental ratio= 331.6 ± 72.1 (21.75%)			mean elemental ratio= 323.0 ± 52.33 (16.2%)		

B.2 Thin targets

B.2.1 The element pair potassium-calcium

B.2.1.1 Potassium as major component

The mean elemental ratio is given by $\overline{R} \times \frac{\sigma_{Ca}}{\sigma_K} = \overline{R} \times 0.87416$ and the relative precision is derived from the standard deviation of $\overline{R}$

Nominal elemental ratio								
K:Ca (10:1)			K:Ca (20:1)			K:Ca (50:1)		
Y_o(K)	Y_o(Ca)	Count ratio	Y_o(K)	Y_o(Ca)	Count ratio	Y_o(K)	Y_o(Ca)	Count ratio
75740	6224	12.17	78552	3966	19.81	96448	1824	52.86
79680	6475	12.31	77805	3443	22.60	85718	1464	58.55
85260	7440	11.46	68610	3385	20.27	96930	1804	53.73
82512	7172	11.51	72743	3625	20.07	72919	1239	58.85
73290	6147	11.93	71630	3596	19.92	71954	1320	54.51
79338	6263	12.67	59979	3012	19.91	71044	1286	55.24
$\overline{R}$ = mean count ratio = 12.01 Std. deviation ±0.47			$\overline{R}$ = mean count ratio = 20.43 Std. deviation ±1.08			$\overline{R}$ = mean count ratio = 56.36 Std. deviation ±3.01		
mean elemental ratio= 10.5 ± 0.41 (3.91%)			mean elemental ratio= 17.86 ± 0.94 (5.26%)			mean elemental ratio= 49.27 ± 2.63 (5.34%)		

B.2.1 The element pair calcium-potassium.

B.2.1.1 Potassium as major component

The mean elemental ratio is given by $\overline{R} \times \frac{\sigma_{Ca}}{\sigma_K} = \overline{R} \times 0.87416$ and the relative precision is derived from the standard deviation of $\overline{R}$

Nominal elemental ratio								
K:Ca (100:1)			K:Ca (200:1)			K:Ca (500:1)		
Y_o(K)	Y_o(Ca)	Count ratio	Y_o(K)	Y_o(Ca)	Count ratio	Y_o(K)	Y_o(Ca) *(Forced)*	Count ratio
76709	652	117.65	54447	238	228.77	51651	263	196.39
80001	668	119.76	56732	248	228.76	53536	278	192.58
66473	663	100.26	66469	296	224.56	59191	237	249.75
75273	618	121.80	66047	273	241.93	63495	265	239.60
77179	621	124.28	67887	287	236.54	50855	262	194.10
62815	618	101.64	52920	232	228.10	41348	212	195.04
77079	691	111.57	58546	283	206.88			
$\overline{R}$ = mean count ratio = 113.85 Std. deviation ±9.66			$\overline{R}$ = mean count ratio = 227.93 Std. deviation ±11.0			$\overline{R}$ = mean count ratio = 211.24 Std. deviation ±26.13		
mean elemental ratio= 99.53 ± 8.45 (8.49%)			mean elemental ratio= 199.25 ± 9.62 (4.83%)			mean elemental ratio= 184.66 ± 22.84 (12.38%)		

B.2.1 The element pair potassium-calcium

B.2.1.1 Potassium as major component

The mean elemental ratio is given by $\overline{R} \times \frac{\sigma_{Ca}}{\sigma_K} = \overline{R} \times 0.87416$ and the relative precision is derived from the standard deviation of $\overline{R}$

Nominal elemental ratio								
K:Ca (1 000:1)			K:Ca (5 000:1)			K:Ca (10 000:1)		
Y_o(K)	Y_o(Ca) *(Forced)*	Count ratio	Y_o(K)	Y_o(Ca) *(Forced)*	Count ratio	Y_o(K)	Y_o(Ca) *(Forced)*	Count ratio
51452	207	248.6	61659	352	176.0	41388	200	206.9
40692	239	170.2	62601	225	278.2	60790	249	244.1
45779	236	194.0	61396	287	213.9	61973	285	217.4
54472	271	201.0	63849	294	162.1	49532	205	241.6
53405	287	186.1	60842	287	212.0	61973	350	177.1
50970	212	240.4	62192	291	213.7	49528	189	262.1
			54447	238	228.8	45331	202	224.4
			57665	249	231.6	45143	245	184.3
$\overline{R}$ = mean count ratio = 206.7 Std. deviation ±31.1			$\overline{R}$ = mean count ratio = 214.5 Std. deviation ±35.4			$\overline{R}$ = mean count ratio = 219.7 Std. deviation ±29.6		
mean elemental ratio= 180.7 ± 27.2 (15.06%)			mean elemental ratio= 187.5 ± 31.0 (16.52%)			mean elemental ratio= 192.1 ± 25.9 (13.47%)		

B.2.1 The element pair calcium-potassium.

B.2.1.2 Calcium as major component

The mean elemental ratio is given by $\overline{R} \times \frac{\sigma_K}{\sigma_{Ca}} = \overline{R} \times 1.14396$ and the relative precision is derived from the standard deviation of $\overline{R}$

Nominal elemental ratio								
Ca:K (10:1)			Ca:K (20:1)			Ca:K (50:1)		
Y_o(Ca)	Y_o(K)	Count ratio	Y_o(Ca)	Y_o(K)	Count ratio	Y_o(Ca)	Y_o(K)	Count ratio
59353	6048	9.81	48951	2451	19.97	69636	1554	44.81
58208	5983	9.73	56736	2958	19.18	54510	1230	44.321
50745	5055	10.04	46812	2352	19.90	62403	1409	44.29
55059	5472	10.06	51690	2552	20.26	60256	1360	44.31
59116	5915	9.99	47880	2339	20.47	58516	1272	46.0
52532	5201	10.10	54310	2693	20.17	61020	1408	43.34
						69080	1373	50.33
$\overline{R}$ = mean count ratio = 9.63 Std. deviation ±0.15			$\overline{R}$ = mean count ratio = 19.99 Std. deviation ±0.45			$\overline{R}$ = mean count ratio = 51.87 Std. deviation ±2.34		
mean elemental ratio= 11.39 ± 0.17 (1.51%)			mean elemental ratio= 22.87 ± 0.51 (2.23%)			mean elemental ratio= 51.87 ± 2.68 (5.16%)		

B.2.1 The element pair calcium-potassium.

B.2.1.2 Calcium as major component

The mean elemental ratio is given by $\overline{R} \times \frac{\sigma_K}{\sigma_{Ca}} = \overline{R} \times 1.14396$ and the relative precision is derived from the standard deviation of $\overline{R}$

Nominal elemental ratio								
Ca:K (100:1)			Ca:K (200:1)			Ca:K (500:1)		
Y_o(Ca)	Y_o(K)	Count ratio	Y_o(Ca)	Y_o(K)	Count ratio	Y_o(Ca)	Y_o(K) *(Forced)*	Count ratio
54449	584	93.24	55610	298	186.61	45483	204	222.95
54051	638	84.72	55821	303	184.23	40769	282	144.57
57108	582	98.12	56341	266	211.81	45512	297	153.24
53838	586	91.87	56998	306	186.27	43683	242	180.51
54579	579	94.26	60671	304	199.57	42422	242	175.3
65505	630	103.97	52716	288	183.04	43556	241	180.73
60948	624	97.67	50141	263	190.65	49235	223	220.79
57734	612	94.34	41855	223	187.69	41024	229	179.14
$\overline{R}$ = mean count ratio = 94.68 Std. deviation ±5.63			$\overline{R}$ = mean count ratio = 191.23 Std. deviation ±9.77			$\overline{R}$ = mean count ratio = 183.18 Std. deviation ±10.03		
mean elemental ratio= 108.31 ± 6.44 (5.94%)			mean elemental ratio= 218.76 ± 11.18 (5.11%)			mean elemental ratio= 209.55 ± 11.47 (5.47%)		

B.2.1 The element pair calcium-potassium.

B.2.1.2 Calcium as major component

The mean elemental ratio is given by $\overline{R} \times \frac{\sigma_K}{\sigma_{Ca}} = \overline{R} \times 1.14396$ and the relative precision is derived from the standard deviation of $\overline{R}$

Nominal elemental ratio								
Ca:K (1 000:1)			Ca:K (5 000:1)			Ca:K (10 000:1)		
Y_o(Ca)	Y_o(K) *(Forced)*	Count ratio	Y_o(Ca)	Y_o(K) *(Forced)*	Count ratio	Y_o(Ca)	Y_o(K) *(Forced)*	Count ratio
42692	276	154.7	40488	285	142.1	48373	236	205.0
49781	297	167.6	42328	286	148.0	44518	311	143.1
50229	308	163.1	40357	250	161.4	46993	292	160.9
51872	355	146.1	43072	286	150.6	50968	254	180.1
52134	373	139.8	41140	217	189.6	50224	254	197.7
54316	280	194.0	40693	192	211.9	42407	301	140.9
52376	269	194.7	59160	298	198.5	43512	259	168.0
52576	294	178.830	54488	262	207.969	42346	222	190.748
$\overline{R}$ = mean count ratio = 167.3 Std. deviation ±20.6			$\overline{R}$ = mean count ratio = 176.3 Std. deviation ±28.8			$\overline{R}$ = mean count ratio = 173.3 Std. deviation ±24.2		
mean elemental ratio= 191.4 ± 23.6 (12.33%)			mean elemental ratio= 201.6 ± 32.9 (16.33%)			mean elemental ratio= 198.3 ± 27.7 (13.95%)		

B.2.2 The element pair vanadium-chromium

B.2.2.1 Vanadium as major component

The mean elemental ratio is given by $\overline{R} \times \frac{\sigma_{Cr}}{\sigma_V} = \overline{R} \times 0.84068$ and the relative precision is derived from the standard deviation of $\overline{R}$

Nominal elemental ratio								
V:Cr (10:1)			V:Cr (20:1)			V:Cr (50:1)		
Y_o(V)	Y_o(Cr)	Count ratio	Y_o(V)	Y_o(Cr)	Count ratio	Y_o(V)	Y_o(Cr)	Count ratio
152100	13174	11.55	168990	6850	24.69	213091	3321	64.1
142500	11814	12.06	161590	6960	23.2	161731	2651	60.98
135284	11488	11.78	173444	6806	25.51	157102	2442	64.52
145736	12729	11.46	154589	7009	22.08	170121	2781	61.35
120322	10260	11.72	134529	5841	23.04	162592	2672	60.98
124081	10308	12.03						
$\overline{R}$ = mean count ratio = 11.77 Std. deviation ±0.248			$\overline{R}$ = mean count ratio = 23.7 Std. deviation ±1.38			$\overline{R}$ = mean count ratio = 62.38 Std. deviation ±1.77		
mean elemental ratio= 9.89 ± 0.208 (2.11%)			mean elemental ratio= 19.93 ± 1.16 (5.81%)			mean elemental ratio= 52.45 ± 1.45 (2.84%)		

B.2.2 The element pair vanadium-chromium

B.2.2.1 Vanadium as major component

The mean elemental ratio is given by $\overline{R} \times \frac{\sigma_{Cr}}{\sigma_V} = \overline{R} \times 0.84068$ and the relative precision is derived from the standard deviation of $\overline{R}$

Nominal elemental ratio								
V:Cr (100:1)			V:Cr (200:1)			V:Cr (500:1)		
Y_o(V)	Y_o(Cr)	Count ratio	Y_o(V)	Y_o(Cr)	Count ratio	Y_o(V)	Y_o(Cr) *(Forced)*	Count ratio
169590	1350	125.62	169607	624	271.74	210067	724	289.86
173358	1308	132.54	164138	708	232.56	223365	748	298.62
180596	1320	136.8	204995	800	256.24	239045	834	286.53
171870	1393	123.46	141565	550	257.39	168906	810	208.53
221143	1650	134.05	150667	592	253.67	240236	917	261.98
166397	1371	121.36	230376	946	243.31	185915	897	207.47
$\overline{R}$ = mean count ratio = 128.97 Std. deviation ±6.31			$\overline{R}$ = mean count ratio = 252.49 Std. deviation ±13.35			$\overline{R}$ = mean count ratio = 258.83 Std. deviation ±41.21		
mean elemental ratio= 108.42 ± 5.31 (4.9%)			mean elemental ratio= 212.26 ± 11.23 (5.29%)			mean elemental ratio= 217.59 ± 34.64 (15.92%)		

B.2.2 The element pair vanadium-chromium

B.2.2.1 Vanadium as major component

The mean elemental ratio is given by $\overline{R} \times \frac{\sigma_{Cr}}{\sigma_K} = \overline{R} \times 0.84068$ and the relative precision is derived from the standard deviation of $\overline{R}$

Nominal elemental ratio								
V:Cr (1 000:1)			V:Cr (5 000:1)			V:Cr (10 000:1)		
Y_o(V)	Y_o(Cr) *(Forced)*	Count ratio	Y_o(V)	Y_o(Cr) *(Forced)*	Count ratio	Y_o(V)	Y_o(Cr) *(Forced)*	Count ratio
141954	529	268.1	108844	318	342.5	102553	388	264.3
128452	485	264.8	101073	361	280.1	152961	635	240.9
143549	477	301.2	95237	473	201.2	143358	308	465.4
173012	698	247.9	148748	397	374.5	153389	430	356.7
168515	594	284.1	167938	586	286.5	153356	463	331.2
142554	402	354.6	123669	467	264.6	127032	280	453.7
			24948	109	228.8	116959	384	304.6
$\overline{R}$ = mean count ratio = 286.8			$\overline{R}$ = mean count ratio = 282.6			$\overline{R}$ = mean count ratio = 345.3		
Std. deviation ±37.84			Std. deviation ±60.41			Std. deviation ±87.21		
mean elemental ratio= 241.1 ± 31.82 (13.20%)			mean elemental ratio= 237.58 ± 50.79 (21.38%)			mean elemental ratio= 290.25 ± 73.31 (25.26%)		

B.2.2 The element pair vanadium-chromium

B.2.2.2 Chromium as major component

The mean elemental ratio is given by $\overline{R} \times \frac{\sigma_V}{\sigma_{Cr}} = \overline{R} \times 1.18952$ and the relative precision is derived from the standard deviation of $\overline{R}$

Nominal elemental ratio								
Cr:V (10:1)			Cr:V (20:1)			Cr:V (50:1)		
Y_o(Cr)	Y_o(V)	Count ratio	Y_o(Cr)	Y_o(V)	Count ratio	Y_o(Cr)	Y_o(V)	Count ratio
84548	10217	8.28	135472	7438	18.22	226736	4846	46.73
82477	10274	8.03	143680	7796	18.42	193641	4220	45.89
77659	9466	8.20	138568	7168	19.34	195172	4165	46.86
87780	10513	8.35	135003	7314	18.45	190759	4025	47.39
89798	10761	8.34	121345	6548	18.52	198424	4298	46.02
			108776	5864	18.55	172688	3909	44.25
$\overline{R}$ = mean count ratio = 8.24			$\overline{R}$ = mean count ratio = 18.58			$\overline{R}$ = mean count ratio = 46.19		
Std. deviation ±0.132			Std. deviation ±0.39			Std. deviation ±1.103		
mean elemental ratio= 9.8 ± 0.157 (1.6%)			mean elemental ratio= $22.1 \pm .464$ (2.1%)			mean elemental ratio= 54.94 ± 1.31 (2.39%)		

B.2.2 The element pair vanadium-chromium

B.2.2.2 Chromium as major component

The mean elemental ratio is given by $\overline{R} \times \frac{\sigma_V}{\sigma_{Cr}} = \overline{R} \times 1.18952$ and the relative precision is derived from the standard deviation of $\overline{R}$

Nominal elemental ratio								
Cr:V (100:1)			Cr:V (200:1)			Cr:V (500:1)		
Y_o(Cr)	Y_o(V)	Count ratio	Y_o(Cr)	Y_o(V)	Count ratio	Y_o(Cr)	Y_o(V) *(Forced)*	Count ratio
152021	1765	86.13	123975	670	185.04	44231	141	313.48
155956	1849	84.35	77528	400	193.82	51290	138	337.84
175280	2240	78.25	77233	428	180.45	59208	168	352.11
156249	2130	73.36	84796	510	166.27	101716	250	406.50
174977	2390	73.21	117502	595	197.48	99052	338	495.05
172320	2310	74.60	127747	678	188.42	95388	250	381.68
			121718	684	177.95	168959	338	500.0
						154498	318	485.44
$\overline{R}$ = mean count ratio = 78.32 Std. deviation ±5.69			$\overline{R}$ = mean count ratio = 184.20 Std. deviation ±10.51			$\overline{R}$ = mean count ratio = 409.01 Std. deviation ±75.31		
mean elemental ratio= 93.16 ± 6.77 (7.27%)			mean elemental ratio= 219.11 ± 12.5 (5.7%)			mean elemental ratio= 486.53 ± 89.59 (18.41%)		

B.2.2 The element pair vanadium-chromium

B.2.2.2 Chromium as major component

The mean elemental ratio is given by $\overline{R} \times \frac{\sigma_V}{\sigma_{Cr}} = \overline{R} \times 1.18952$ and the relative precision is derived from the standard deviation of $\overline{R}$

Nominal elemental ratio								
Cr:V (1 000:1)			Cr:V (5 000:1)			Cr:V (10 000:1)		
Y_o(Cr)	Y_o(V) *(Forced)*	Count ratio	Y_o(Cr)	Y_o(V) *(Forced)*	Count ratio	Y_o(Cr)	Y_o(V) *(Forced)*	Count ratio
84865	423	200.8	86543	276	314.5	128506	299	429.8
99855	357	279.3	108834	323	336.7	91389	565	161.8
104030	369	281.7	112019	342	327.9	91854	241	381.1
91661	411	223.2	107440	328	326.8	107173	256	418.6
152067	457	332.2	164839	505	253.8	133444	346	385.7
154745	421	367.6	150190	591	386.1	154065	341	451.8
			107336	278	283.3	191369	330	434.9
$\overline{R}$ = mean count ratio = 280.8			$\overline{R}$ = mean count ratio = 318.4			$\overline{R}$ = mean count ratio = 380.5		
Std. deviation ±63.1			Std. deviation ±41.83			Std. deviation ±99.82		
mean elemental ratio= 334.04 ± 75.05 (22.47%)			mean elemental ratio= 378.78 ± 49.76 (13.14%)			mean elemental ratio= 452.6 ± 118.7 (26.23%)		